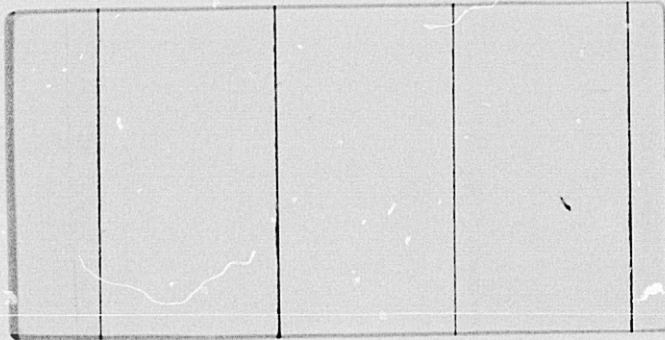


General Disclaimer

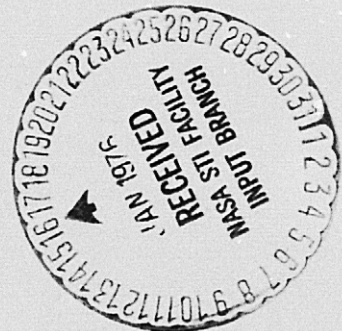
One or more of the Following Statements may affect this Document

- This document has been reproduced from the best copy furnished by the organizational source. It is being released in the interest of making available as much information as possible.
- This document may contain data, which exceeds the sheet parameters. It was furnished in this condition by the organizational source and is the best copy available.
- This document may contain tone-on-tone or color graphs, charts and/or pictures, which have been reproduced in black and white.
- This document is paginated as submitted by the original source.
- Portions of this document are not fully legible due to the historical nature of some of the material. However, it is the best reproduction available from the original submission.



(NASA-CR-145986) ANALYSIS OF DATA FROM THE
LOCKHEED EXPERIMENT ON ATS-5 Final Report
(Lockheed Missiles and Space Co.) 101 p HC
\$5.50 CACL 04A

N76-15705
THRU
N76-15708
Unclas
08081
G3/46



LOCKHEED

MISSILES & SPACE COMPANY, INC. • SUNNYVALE, CALIFORNIA

A SUBSIDIARY OF LOCKHEED AIRCRAFT CORPORATION

LMSC/D460734

2 September 1975

FINAL REPORT

"ANALYSIS OF DATA FROM THE
LOCKHEED EXPERIMENT ON ATS-5"

Contract NASw 2656

Prepared by:

Dr. Richard D. Sharp
Principal Investigator
Space Sciences Laboratory
Lockheed Palo Alto Research Laboratory
Lockheed Missiles & Space Company, Inc.
3251 Hanover Street
Palo Alto, California 94304

TABLE OF CONTENTS

	<u>Title</u>	<u>Page</u>
Discussion.....		1
 <u>Appendices</u>		
A	A Relationship between Synchronous-Altitude Electron Fluxes and the Auroral Electrojet, by R. D. Sharp, E. G. Shelley, and G. Rostoker.....	A-1 <i>D1</i>
B	Coordinated ATS-5 Electron Flux and Simultaneous Auroral Observations, by S. B. Mende and E. G. Shelley	B-1 <i>D2</i>
C	ATS-5 Observations of Plasma Sheet Particles before the Expansion-Phase Onset, by K. Fujii, A. Nishida, R. D. Sharp, and E. G. Shelley.....	C-1 <i>D3</i>
D	A Comprehensive Study of Substorm Sequences on September 8, 1969 (Abstract), by G. Rostoker, S.-I. Akasofu, H. Fukunishi, E. W. Hones, Jr., L. J. Lanzerotti, C. G. MacLennan, R. L. McPherron, R. D. Sharp, and R. G. Wiens.....	D-1 <i>X</i>
E	Simultaneous Observations of Synchronous-Altitude Particle Fluxes and the Auroral Electrojet (Abstract), by R. D. Sharp, E. G. Shelley, and G. Rostoker.....	E-1 <i>X</i>

FINAL REPORT

"ANALYSIS OF DATA FROM THE LOCKHEED EXPERIMENT ON ATS-5"

Contract NASw 2656

This is a final report of a program for the analysis of the data from the Lockheed Experiment on ATS-5. The principal results of this study are contained in three publications which are in various stages of publication.

1. "A Relationship between Synchronous-Altitude Electron Fluxes and the Auroral Electrojet," by R. D. Sharp, E. G. Shelley, and G. Rostoker, published in the Journal of Geophysical Research, Vol. 80, p. 2319, 1975.
2. "Coordinated ATS-5 Electron Flux and Simultaneous Auroral Observations," by S. B. Mende and E. G. Shelley, submitted to the Journal of Geophysical Research, 1975.
3. "ATS-5 Observations of Plasma Sheet Particles before the Expansion-Phase Onset," by K. Fujii, A. Nishida, R. D. Sharp, and E. G. Shelley, submitted to Planetary and Space Sciences, 1975.

In addition, two invited papers were presented at the Topical Conference on Electrodynamics of Substorms and Magnetic Storms, Bryce Mountain, Virginia, June 11-14, 1974.

1. "A Comprehensive Study of Substorm Sequences on September 8, 1969," by G. Rostoker, S.-I. Akasofu, H. Fukunishi, E. W. Hones, Jr., L. J. Lanzerotti, C. G. MacLennan, R. L. McPherron, R. D. Sharp, and R. G. Wiens.

2. Simultaneous Observations of Synchronous-Altitude Particle Fluxes and the Auroral Electrojet," by R. D. Sharp, E. G. Shelley, and G. Rostoker.

The abstracts of these invited papers were published in EOS, Vol. 55, pages 988 and 1013, 1974. Copies of the three publications and the abstracts of the two invited papers are included in the Appendices.

In addition to the published results described above, we have also provided data to several investigators with whom we are cooperating on the study of various other events. These include Dr. E. W. Hones of Los Alamos Scientific Laboratory, Prof. R. H. Eather of Boston College, Dr. S. B. Mende of Lockheed Palo Alto Research Laboratory, and Mr. T. Hughes of the University of Alberta. Mr. Hughes is utilizing the results of our cooperative study for his Ph.D. thesis under Professor Gordon Rostoker and selected results from this work are also expected to be submitted for publication.

R. D. Sharp

R. D. Sharp, Principal Investigator
Lockheed Palo Alto Research Laboratory

N76-15706

Accepted for publication in the
Journal of Geophysical Research

-1-

A P P E N D I X A

BRIEF REPORT

A RELATIONSHIP BETWEEN SYNCHRONOUS-ALTITUDE
ELECTRON FLUXES AND THE AURORAL ELECTROJET

R. D. Sharp and E. G. Shelley
Lockheed Palo Alto Research Laboratory
Palo Alto, California 94304

and

G. Rostoker
The University of Alberta
Edmonton 7, Alberta, Canada

October 1974

(Revised January 1975)

PRECEDING PAGE BLANK NOT FILMED

BRIEF REPORT

A RELATIONSHIP BETWEEN SYNCHRONOUS-ALTITUDE
ELECTRON FLUXES AND THE AURORAL ELECTROJET

By

R. D. Sharp and E. G. Shelley
Lockheed Palo Alto Research Laboratory
Palo Alto, California 94304

And

G. Rostoker
The University of Alberta
Edmonton 7, Alberta, Canada

ABSTRACT

Simultaneous observations during four substorms are reported from the Lockheed auroral particle spectrometer on ATS-5 and the University of Alberta meridian magnetometer chain. During the four events studied, there was a good correlation between the magnitude of the trapped electron fluxes in the energy range from 1.8 to 53 keV and the magnitude of the electrojet current as measured by a station in the magnetometer chain at a latitude close to that expected for the ATS conjugate point. A model electrojet is constructed based on the work of Coroniti and Kennel [1972] which gives a good absolute agreement between the two measured quantities. The results are consistent with the convection electric field remaining approximately constant during a substantial portion of each of the substorms studied. The temporal variations of the electrojet were apparently controlled by conductivity changes in the ionosphere as determined by the precipitating auroral electrons.

INTRODUCTION

In the course of a cooperative study of the data from the Lockheed auroral particle spectrometer on ATS-5 and the University of Alberta meridian magnetometer chain in central Canada, an interesting quantitative relationship was discovered between the magnitude of the auroral electrojet and the character of the electron fluxes at ATS. This report will focus on this relationship. We will show data from the midnight sector during the expansive phases of four substorms. More complete descriptions of these events have been presented by Kisabeth and Rostoker [1971, 1974], Kisabeth [1972], and Rostoker et al. [1974].

The Lockheed auroral particle experiment measures electrons and protons in the range from about 1-50 keV. The spectrometer and the data analysis procedures utilized to obtain the ambient plasma properties have been described by Sharp et al. [1971, 1970], Shelley et al. [1971], and Mende et al. [1972]. The spectrometer is oriented along the spin axis of the spacecraft and was sampling trapped particles with equatorial pitch angles in the range from about 20° to 50° during the events studied here.

The foot of the field line passing through ATS-5 maps into central Canada near Lynn Lake, Saskatchewan, which is about 15° east of the magnetometer chain. The four events to be described are the only events so far analyzed and were selected on the basis of substantial electrojet currents with a considerable longitudinal extent (based on the ground magnetometer data) in order to minimize the uncertainties arising from this longitudinal separation. Local midnight at the satellite is approximately 0700 UT.

RESULTS

We first consider the substorm of 1 September 1970 [Kissbeth and Rostoker, 1974]. The time of onset of the expansive phase of the substorm was determined to be 0654 from the ground-based data. The onset occurred at 64° invariant latitude which is equatorward of the nominal location of the ATS-5 field line as determined from average models of the geomagnetic field [Fairfield, 1968]. There were no significant effects observed in the particle data at ATS at the time of onset [Rostoker et al., 1974]. The initial increase was observed in all electron channels simultaneously at 0658. We infer from this lack of energy dispersion that the flux increase was not due to a longitudinally drifting plasma cloud intercepting the spacecraft but resulted from a radial motion or a local acceleration.

The principle effect observed in the ground data during the period between the onset of the substorm and the observed flux increase at ATS-5 was a poleward propagation of the disturbance. The northern border reached $66\frac{1}{2}^{\circ}$ invariant latitude at the time of the flux increase and a plausible interpretation of this is that a radially outward propagating disturbance had intercepted the spacecraft at this time [Rostoker et al., 1974].

This establishes the location of the ATS field line at this point in the substorm. We now examine the time dependence of the electrojet at this location. The upper panel of Fig. 1 shows the variation in the horizontal component of the geomagnetic field at the closest station in the magnetometer chain (Port Chipewyan, invariant latitude = 66.5°). We see a generally increasing westward electrojet in the period after the onset of the substorm, reaching its maximum value at about 0705. The lower panels of Fig. 1 show the characteristics of the electron

fluxes at ATS in the range from 1.8 to 53 keV during this period. The omnidirectional energy flux under the assumption of isotropy and the average electron energy (flux weighted average) are illustrated. One sees that the flux is generally increasing in intensity and hardness and reaches a plateau in both these parameters at about the same time as the plateau in the electrojet current is achieved. This suggests the possibility of a quantitative relationship between these parameters. A detailed model is required in order to test this hypothesis.

The model electrojet we have utilized is based on the work of Coroniti and Kennel [1972]. It assumes a primary, quasi-constant westward electric field (the convection field) which drives a northward Hall current in the ionosphere. This Hall current closes with field aligned currents which are interrupted when they exceed the threshold for electrostatic wave instabilities. The lower ionosphere then polarizes creating a southward electric field whose Pederson current balances the northward Hall current. This is the southward field which is the commonly observed feature of the breakup phase of the substorm. It derives from, and is proportional to, the primary convection field. The large Hall current driven by this southward field is the principal contributor to the westward electrojet. In the limit of very large field-aligned resistivity, the electrojet current density I_y is given by

$$I_y = E_y (\Sigma_P + \Sigma_H^2 / \Sigma_P)$$

where E_y is the westward convection field, and Σ_P and Σ_H are the height-integrated Pederson and Hall conductivities, respectively. In this limit, the

enhanced electrojet current is referred to as a Cowling current and the quantity in brackets is known as the Cowling conductivity, Σ_c . It can be calculated from the precipitating energetic electron spectrum which we can estimate from the measured trapped electrons at ATS.

The conductivity at an altitude z , $\sigma(z)$, is proportional to the electron density $n(z)$. Under equilibrium conditions

$$n(z) = [q(z)/\alpha(z)]^{1/2}$$

where $\alpha(z)$ = the recombination coefficient and $q(z)$ = the ionization rate due to the primary energetic electrons. For $n(z)$ we use the results of Cladis et al. [1973] who calculated electron density profiles for a series of primary energetic electron spectrums of the form

$$J(E) = A E \exp(-E/E_0)$$

where $J(E)$ is the electron differential number flux, E is the electron energy and E_0 is an energy parameter. This distribution has a peak intensity at energy E_0 and an average energy \bar{E} equal to $2E_0$. The calculations were performed with the Lockheed computer program AURORA which computes the energy deposition of the primary beam as a function of altitude. The theoretical basis for this program has been described by Walt et al. [1968]. It solves the appropriate Fokker-Planck diffusion equation numerically taking into account atmospheric scattering, electron energy loss and the mirroring effect of the geomagnetic field. An isotropic pitch-angle distribution was assumed and experimental values

of $\alpha(z)$ were utilized. These $\alpha(z)$ values are summarized in Watt et al. [1974] by the solid curve in their Figure 10. The model atmosphere used was that of Anderson and Francis [1966].

The Pederson and Hall conductivities $\sigma(z) = k(z)n(z)$ were calculated by Cladis et al. [1974] utilizing the method of Kennel and Rees [1972]. From their results, and the electron density profiles, the height-integrated Hall and Pederson conductivities can be computed as a function of E_0

$$\Sigma = \int \left(\frac{q(z, E_0)}{\alpha(z)} \right)^{1/2} k(z) dz$$

Since the ionization source term $q(z, E_0)$ is proportional to the total precipitated energy flux of the primary spectrum $\Phi = \pi \int E J(E) dE$, we can write $q(z, E_0) = \Phi \cdot f(z, E_0)$ and the quantity

$$\Sigma/\Phi^{1/2} = \int [f(z, E_0)/\alpha(z)]^{1/2} k(z) dz$$

is only a function of E_0 . $\Sigma_P/\Phi^{1/2}$ and $\Sigma_H/\Phi^{1/2}$ were evaluated from this expression at several values of E_0 and combined as indicated above to yield $\Sigma_c/\Phi^{1/2}$. A plot of this quantity versus the average energy of the primary electron spectrum, \bar{E} , is given in Figure 2.

For the purposes of this comparison we have approximated Φ and \bar{E} by the measured values at ATS in the energy range from 1.8 to 53 keV. This effectively assumes that strong pitch-angle diffusion results in an isotropic pitch-angle distribution throughout this period. From the measurements, taken every 5.1 seconds, we have computed the energy flux and the average energy as described in the Appendix of Mende et al. [1972]. Then by interpolating in Figure 2, we

obtained Σ_c . In order to further calculate the perturbation in the horizontal component of the geomagnetic field to compare with the ground-based magnetometer observations we need to assume a model current system and a value for the convection electric field. We utilized the current system of Bonnevier et al. [1970] for a conducting earth below a depth of 100 km with the arbitrary parameters of a 5° latitudinal width, and a 20° longitudinal extent. We assumed this system was centered on the magnetometer station of interest. We further assumed a constant westward electric field over the period of the substorm and used the strength of that field as a free parameter to fit the model calculation to the observed magnetometer data.

The .5-degree latitudinal width is reasonably representative of the cases studied. Also, during these four events the magnetometer station with which we made the comparison was usually within the full width at half maximum of the experimentally determined latitudinal profile of ΔH , in which case for a latitudinally uniform electrojet the corrections for the fact that the actual electrojet was not necessarily centered on this station are less than a factor of 2. For this simplified model no attempt has been made to put in a time dependence for the electrojet width, nor a latitude dependence to the current density.

The assumption that the precipitating electron flux can be approximated by the measured trapped flux at ATS involves two factors. The first is isotropy of the equatorial pitch angle distribution including the loss cone. This is probably a reasonably good approximation especially during the expansive phase of the substorm. Although there are notable exceptions, the majority of low altitude rocket and satellite measurements report approximate isotropy for the pitch angle distribution of auroral electrons during the more intense

precipitation events [Whalen and McDiarmid, 1969; Craven, 1970; Paschmann et al., 1972]. Recent results from the ATS-6 satellite (C. McIlwain, private communication) indicate that sharply field-aligned electron fluxes are occasionally observed at synchronous altitude. At this time, however, their typical energies, frequency of occurrence and relationship to the substorm expansive phase have not been determined. The second factor is the possibility of various mechanisms operating on the electrons as they travel between the equator and the ionosphere. There is considerable evidence building up that such processes can occasionally be important [Evans, 1969, 1974; Sharp et al., 1971; Block 1972]. In neither of these areas is the available data sufficiently extensive to allow for a quantitative correction to the present calculation, particularly since, as noted above, the effects are probably dependent upon the substorm phase. Thus, in the spirit of a simplified model for a first iteration comparison, we will neglect such effects in the present work.

An estimate of the proton contribution to the conductivity during these events was made on the basis of the measured proton fluxes. It was typically of the order of 10% and was neglected in the present analysis. Refinements in the model should also account for the probable systematic latitudinal motion of the ATS conjugate point during the substorm as well as variations in the location and width of the entire electrojet relative to the conjugate point magnetometer.

The results for the substorm on September 1, 1970 are shown in Figure 3. There is surprisingly good agreement in the shapes of the two curves. The normalization yields an effective westward electric field value of about 10 mV/m.

Also shown in Figure 3 is the interesting temporal correspondence between the period of increasing electrojet current and the period of decreasing inclination of the geomagnetic field. This inclination change is a commonly observed signature of the expansive phase of substorms and marks the reconfiguration of the magneto-

tail field from a tail-like to a more dipole-like geometry. It provides further evidence that we are in the injection sector of the substorm and that the observed particle increases are not the result of a longitudinally drifting cloud.

The next three figures (4, 5, and 6) show similar comparisons for the other three events studied. All show substantial evidence for a quantitative relationship between the ATS energetic electron fluxes and the magnitude of the westward auroral electrojet during the time period after the onset of the expansive phase. On day 166, 1970 (see Figure 4) the best fit was obtained with the station at $\Lambda_L = 64.5^\circ$ which was closest to the latitude at which the substorm was initiated in the Alberta sector so that the data from that station (Fort McMurray) were utilized. The model curve was calculated for an electric field of 7.3 mV/m. One sees that there is rather good agreement between the observations and the model predictions for the first 45 minutes after onset, with increasing deviations at later times as the region of maximum disturbance moves further away from the Alberta line and the foot of the ATS-5 field line. Figure 5 shows the results for day 183, 1970; the model curve assumes an electric field of 8.1 mV/m. There is good agreement between the model calculations and observations for a 45-minute period over the major portion of the event. It is interesting to note that in the period before 0648 UT, there is some disagreement between the observations and model calculations with the model predicting higher electrojet strength. This is perhaps understandable in terms of the fact that this particular substorm was initiated to the east of the Alberta line, and the westward surge did not arrive at the station line until 0643 UT. Thus, in the initial stages of the substorm, there was no westward current flow over the station line and the magnetometers recorded the distant effect of currents to the east. The magnetometers would, therefore, tend to underestimate the strength of the auroral electrojet flow at the longitude of the ATS-5 field line during these early stages of the substorm.

The data on day 195, 1970, are compared with a model curve calculated for an electric field of 5.9 mV/m in Figure 6. The data in this case appear to be less well fit by the model than the other three days presented in this study, although the gross features of the behavior of the electrojet are roughly reproduced. The major deviation from the model prediction is the dip in observed negative ΔH at ~ 0825 UT; however, it is important to point out that this dip is associated with the development of a surge form over the station line to the north of 66.5° . The positive ΔH perturbation which is known to dominate the region equatorward of the surge [Akasofu et al., 1956; Kisabeth and Rostoker, 1973] is thus probably responsible for the observed decrease in negative ΔH at 0825 UT.

CONCLUSIONS

These are relatively new results and this is in the nature of a progress report. Further refinements to the model and the examination of additional events will be undertaken. Our conclusions at this point are that these results support the model of Coroniti and Kennel [1972], at least for limited periods of time around local midnight during substorms. The results are consistent with a quasi-constant electric field averaged over the sensitivity region of the magnetometer with which the comparison was made for a substantial portion of each of the substorms studied. The principal temporal variations in the electrojet during these periods were apparently due to conductivity changes resulting from variations in the electron fluxes. This agrees with the results of Mozer [1971] and Gurnett and Akasofu [1974]. Brekke et al. [1974] on the other hand show examples of substorms in which significant variations in the westward electric field were observed. The results reported here also imply strong (or at least constant) pitch-angle diffusion

over the period of the expansive phases of the substorms studied. The effective westward electric field values obtained by the normalization of the model calculation to the observed electrojet are within the range of values determined by other techniques [Mozer, 1971; Haerendel, 1972].

If future studies confirm that during most substorms the electrojet can generally be represented by such a simple model, then the possibility arises of the more extensive application of this technique to the measurement of electric fields. Measurements of 4278Å and 6300Å emissions with a scanning photometer could be used to estimate the parameters Φ and \bar{E} as is done, for example, by Mende and Eather [1972]. If these data were obtained in conjunction with a sufficiently densely-spaced meridian magnetometer chain to allow the simultaneous determination of the electrojet width and intensity, then continuous electric field measurements might be possible over more extended spatial regions and time periods than are attainable by present techniques. One would expect occasional errors in detail from this method for the variety of reasons discussed above. However, statistically useful data for morphological studies might be obtainable on a long-term basis in this way.

ACKNOWLEDGEMENTS

We would like to thank Dr. R. G. Johnson for his many contributions to the ATS-5 program, Dr. J. B. Cladis for helpful discussions on the conductivity calculations, Mr. T. L. Skillman for providing the ATS-5 magnetometer data, and Mr. D. L. Carr for the computer programming used in the analysis of the particle data. This work has been supported by NASA under contract NASw 2656.

ORIGINAL PAGE IS
OF POOR QUALITY

-14-

REFERENCES

Akasofu, S. I., D. S. Kimball, and C. I. Meng, "Dynamics of the Aurora II. Westward Traveling Surges", J. Atmospheric Terrest. Phys., 27, 173, 1965.

Anderson, A. D., and W. E. Francis, "The Variation of the Neutral Atmospheric Properties with Local Time and Solar Activity from 100 to 100,000 km", J. Atmos. Sci., 23, 110, 1966.

Block, L. P., "Potential Double Layers in the Ionosphere", Cosmic Electrodynamics, 3, 349, 1972.

Bonnevier, B., R. Bostrom and G. Rostoker, "A Three Dimensional Model Current System for Polar Magnetic Substorms", J. Geophys. Res., 75, 107, 1970.

Brekke, A., J. R. Doupnik, and P. M. Banks, "Incoherent Scatter Measurements of E Region Conductivities and Currents in the Auroral Zone," J. Geophys. Res., 79, 3773, 1974.

Cladis, J. B., G. T. Davidson, W. E. Francis, L. L. Newkirk and M. Walt, "Ionospheric Disturbances Affecting Radio Wave Propagation", Defense Nuclear Agency Report #DNA-3103F, August 1973.

Cladis, J. B., G. T. Davidson, W. E. Francis, L. L. Newkirk and M. Walt, "Investigation of Phenomena Affecting Auroral Ionosphere", Defense Nuclear Agency Report #DNA-3327F, May 1974.

Coroniti, F. V. and C. F. Kennel, "Polarization of the Auroral Electrojet" J. Geophys. Res., 77, 2835, 1972.

Craven, J. D., "A Survey of Low-Energy ($E > 5$ keV) Electron Energy Fluxes Over the Northern Auroral Regions with Satellite Injun 4", J. Geophys. Res., 75, 2468, 1970.

Evans, D. S., "Fine Structure in the Energy Spectrum of Low Energy Auroral Electrons", in Atmospheric Emissions, edited by B. M. McCormac and A. Omholt. Van Nostrand-Reinhold Co., N. Y., p. 107, 1969.

Evans, D. S., "Precipitating Electron Fluxes Formed by a Magnetic Field Aligned Potential Difference", J. Geophys. Res., 79, 2853, 1974.

Fairfield, D. H., "Average Magnetic Field Configuration of the Outer Magnetosphere", J. Geophys. Res., 73, 7329, 1968.

Gurnett, D. A., S. I. Akasofu, "Electric and Magnetic Field Observations During a Substorm on February 24, 1970", J. Geophys. Res., 79, 3197, 1974.

Haerendel, G., "Electric Fields and Their Effects in the Ionosphere", in Solar Terrestrial Physics/1970, Ed. by E. R. Dyer, Part IV, p. 87, 1972.

Kennel, C. F., and M. H. Rees, "Dayside Auroral Oval Plasma Density and Conductivity Enhancements due to Magnetsheath Electron Precipitation", J. Geophys. Res., 77, 2294, 1972.

Kisabeth, J. L., "The Dynamical Development of the Polar Electrojets", PhD Thesis Dept. of Physics, University of Alberta, Edmonton, Alberta, Canada, 1972.

Kisabeth, J. L., and G. Rostoker, "Development of the Polar Electrojet During Polar Magnetic Substorms", J. Geophys. Res., 76, 6815, 1971.

Kisabeth, J. L., and G. Rostoker, "Current Flow in Auroral Loops and Surges Inferred from Ground Based Magnetic Observations", J. Geophys. Res., 78, 5573, 1973.

Kisabeth, J. L., and G. Rostoker, "The Expansive Phase of Magnetospheric Substorms, I. Development of the Auroral Electrojets and Auroral Arc Configuration During a Substorm", J. Geophys. Res., 79, 972, 1974.

Mende, S. B., and R. H. Eather, "Photometric Auroral Particle Measurements", in Earth's Magnetospheric Processes, B. M. McCormac, ed., D. Reidel Publ. Co., Dordrecht-Holland, pp. 179-186, 1972.

ORIGINAL PAGE IS
OF POOR QUALITY

Mende, S. B., R. D. Sharp, E. G. Shelley, G. Haerendel and E. W. Hones, "Coordinated Observations of the Magnetosphere: The Development of a Substorm", J. Geophys. Res., 77, 4682, 1972.

Mozer, F. S., "Origin and Effects of Electric Fields During Isolated Magnetospheric Substorms", J. Geophys. Res., 76, 7595, 1971.

Paschmann, G., R. G. Johnson, R. D. Sharp and E. G. Shelley, "Angular Distributions of Auroral Electrons in the Energy Range 0.8 to 16 keV", J. Geophys. Res., 77, 6111, 1972.

Rostoker, G., J. L. Kisabeth, R. D. Sharp and E. G. Shelley, "The Expansive Phase of Magnetospheric Substorms II. The Response at Synchronous Altitude of Particles of Different Energy Ranges", Submitted to the J. Geophys. Res., 1974.

Sharp, R. D., D. L. Carr, R. G. Johnson and E. G. Shelley, "Coordinated Auroral-Electron Observations from a Synchronous and a Polar Satellite", J. Geophys. Res., 76, 7669, 1971.

Sharp, R. D., E. G. Shelley, R. G. Johnson and G. Paschmann, "Preliminary Results of a Low-Energy Particle Survey at Synchronous Altitude", J. Geophys. Res., 75, 6092, 1970.

Shelley, E. G., R. G. Johnson and R. D. Sharp, "Plasma Sheet Convection Velocities Inferred from Electron Flux Measurements at Synchronous Altitude", Radio Sci., 6, 305, 1971.

Walt, M., W. M. McDonald and W. E. Francis, "Penetration of Auroral Electrons into the Atmosphere", in Physics of the Magnetosphere, Ed. R. Carovillano and J. F. McClay, Reinhold, N. Y., p. 534, 1968.

Watt, T. M., L. L. Newkirk and E. G. Shelley, "Joint Radar/Satellite Determination of Effective Recombination Coefficient in the Auroral E Region", J. Geophys. Res., 1974 (in press).

Whalen, B. A. and I. B. McDiarmid, "Summary of Rocket Measurements of Auroral Particle Precipitation", in Atmospheric Emissions, Ed. by B. M. McCormac and A. Omholt, Van Nostrand-Reinhold Co., N. Y., p. 93, 1969.

FIGURE CAPTIONS

FIGURE 1 Magnetometer data from Fort Chipewyan, Canada, and ATS-5 electron flux measurements on September 1, 1970. The magnetograms for this day originally appeared in Kisabeth and Rostoker, [1974].

FIGURE 2 Cowling conductivity per unit energy flux to the one half power as a function of the average energy of the precipitating electrons.

FIGURE 3 Lower panel: Model electrojet for a westward electric field of 9.9 mV/m compared with the magnetometer data of Figure 1.

Upper panel: The direction of the magnetic field at ATS-5. Data courtesy of T. Skillman.

FIGURE 4 Data for June 15, 1970 in a format similar to Figure 3. The assumed westward electric field was 7.2 mV/m. The magnetograms for this day originally appeared in Kisabeth and Rostoker, [1971].

FIGURE 5 Data for July 2, 1970 in a format similar to Figure 3. The assumed westward electric field was 8.1 mV/m. The magnetograms for this day originally appeared in Kisabeth and Rostoker, [1971].

FIGURE 6 Data for July 14, 1970 in a format similar to Figure 3. The assumed westward electric field was 5.9 mV/m. The magnetograms for this day originally appeared in Kisabeth [1972].

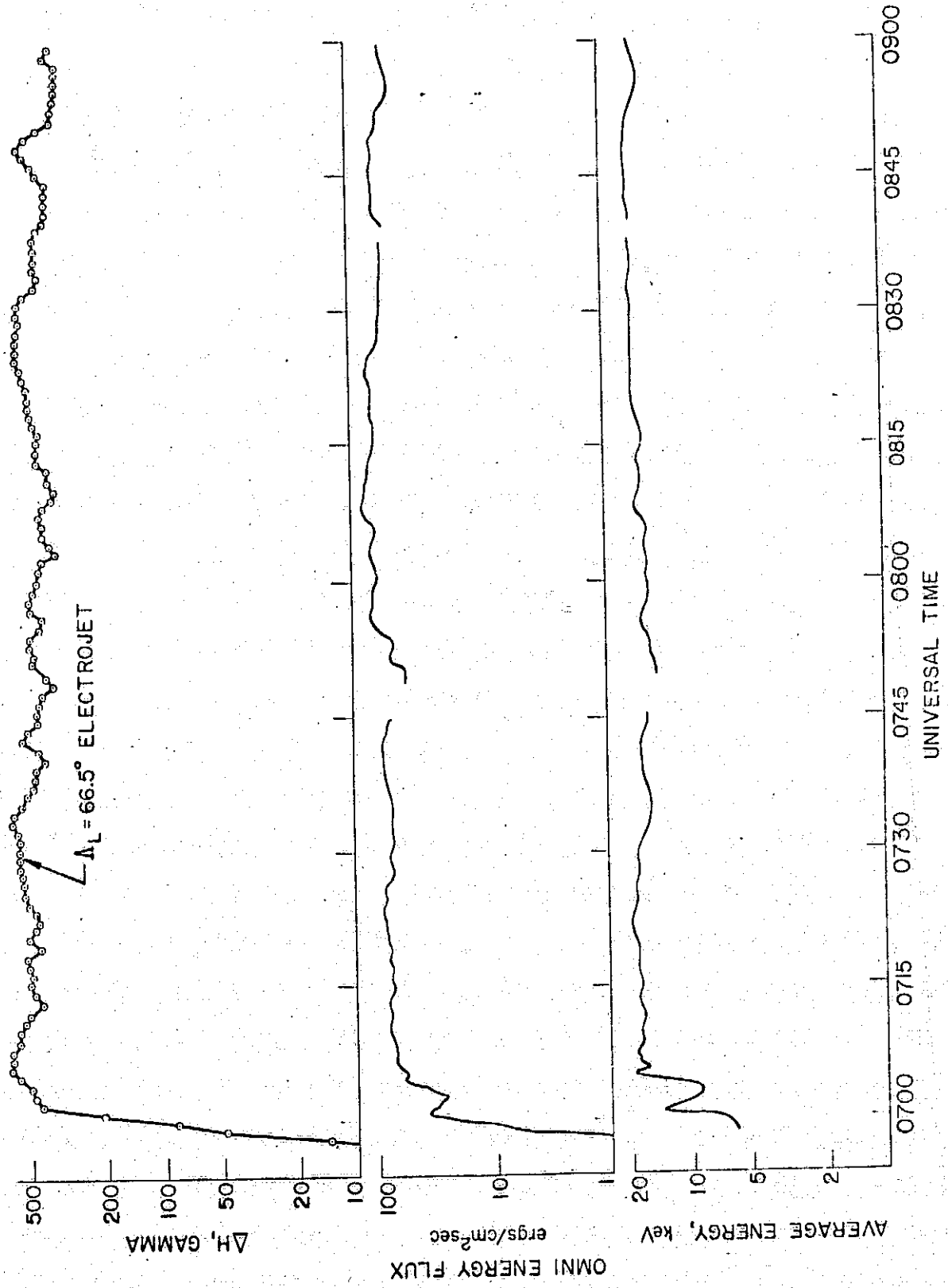


FIGURE 1

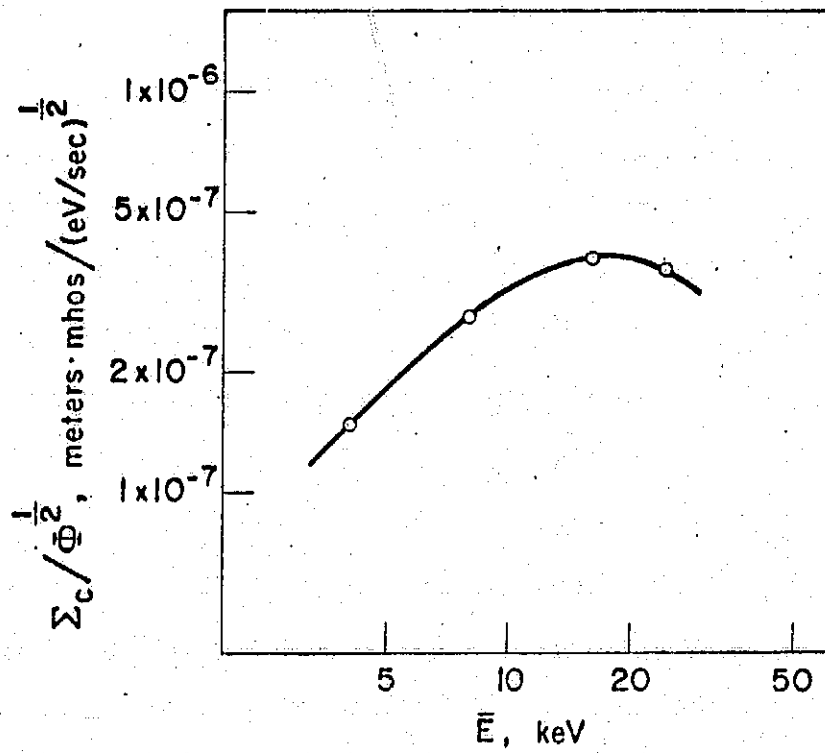


FIGURE 2

PRECEDING PAGE BLANK NOT FILMED

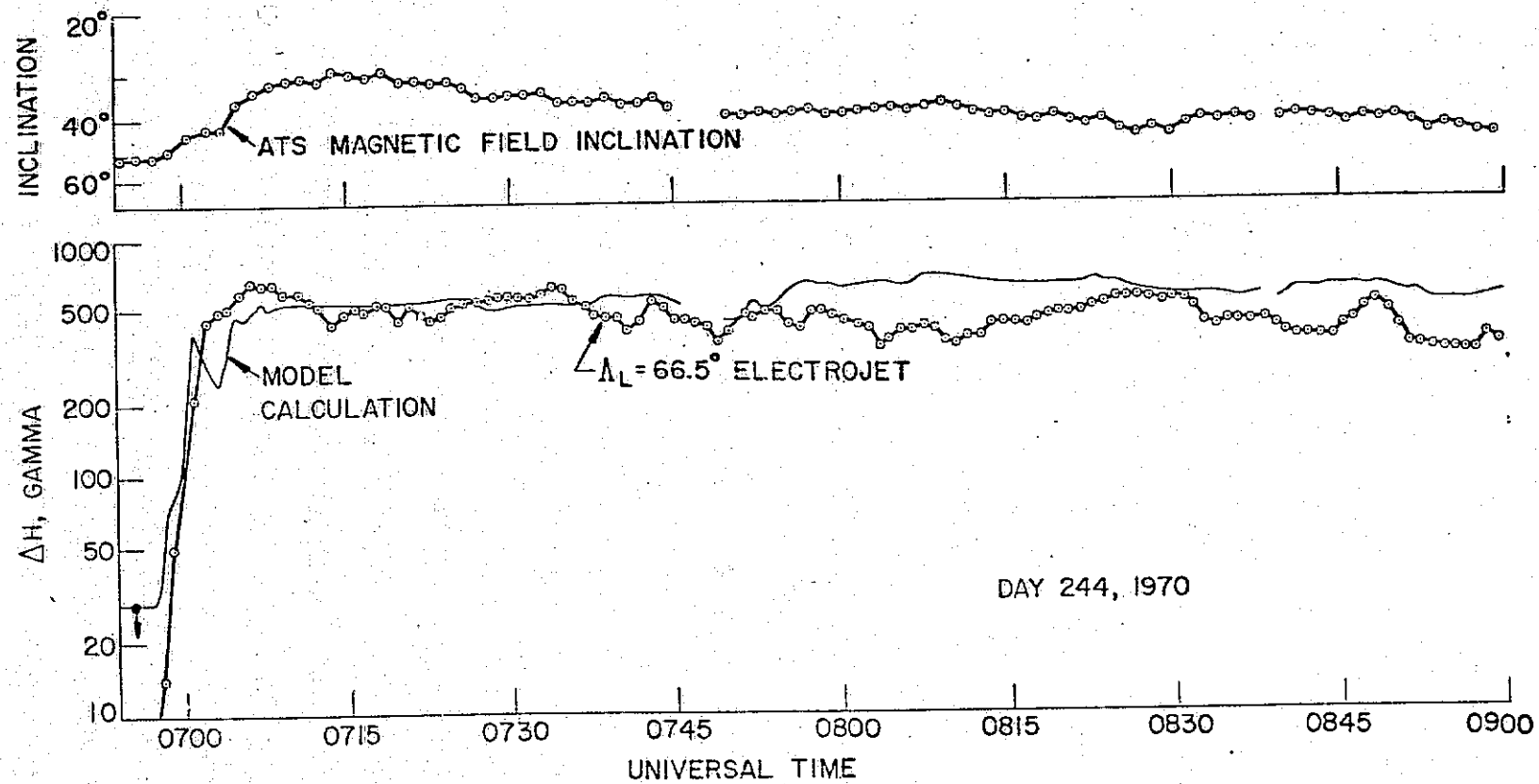


FIGURE 3

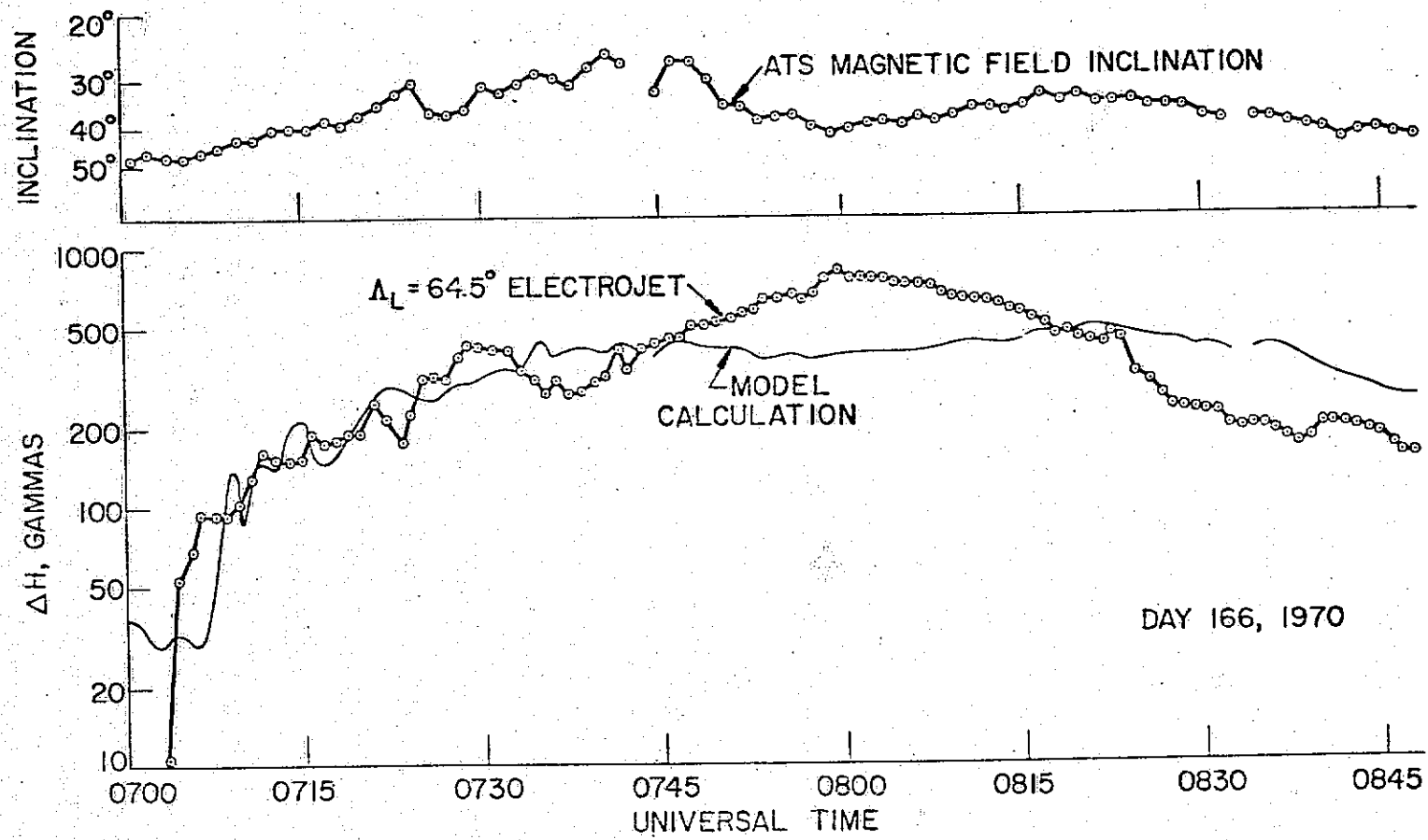


FIGURE 4

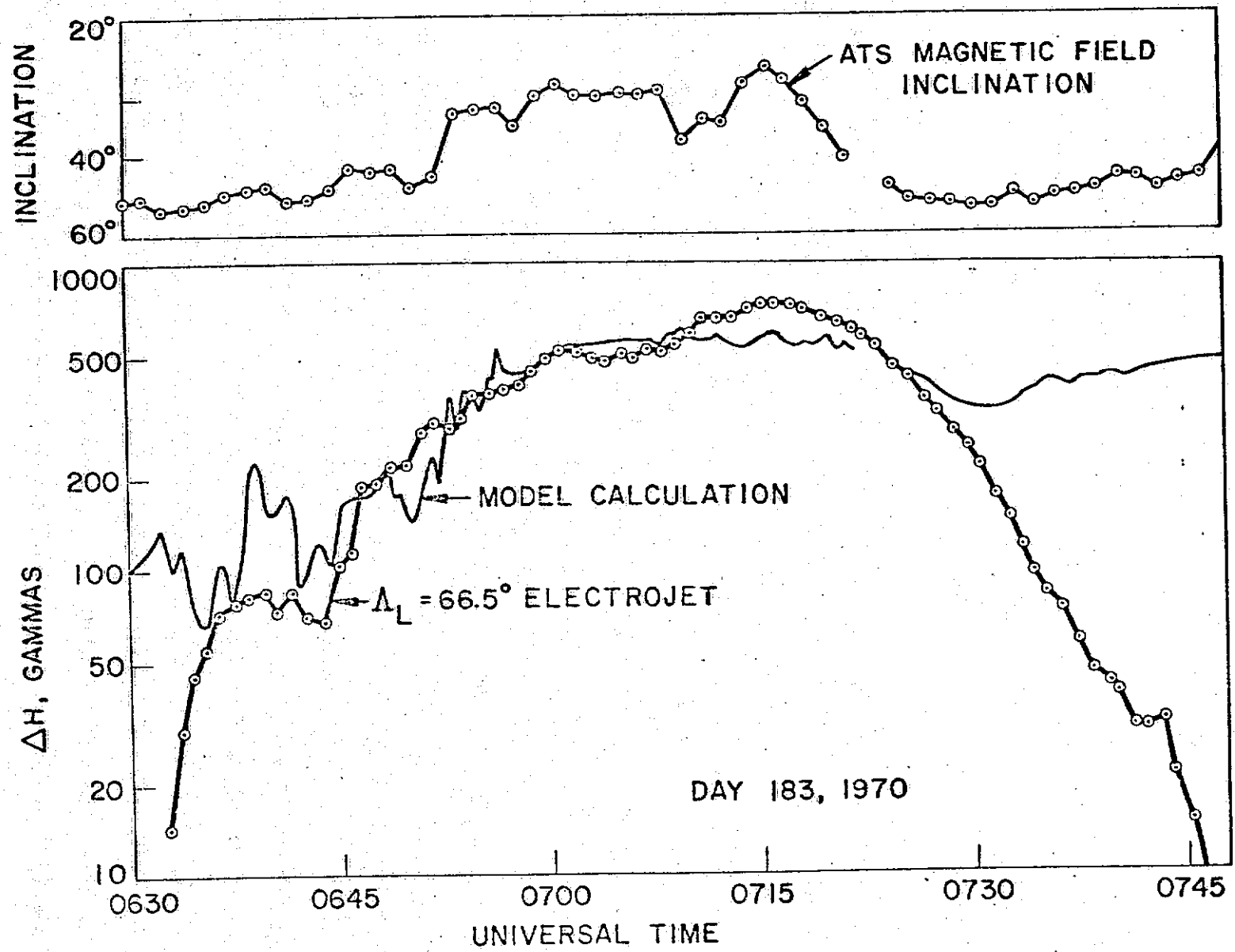


FIGURE 5

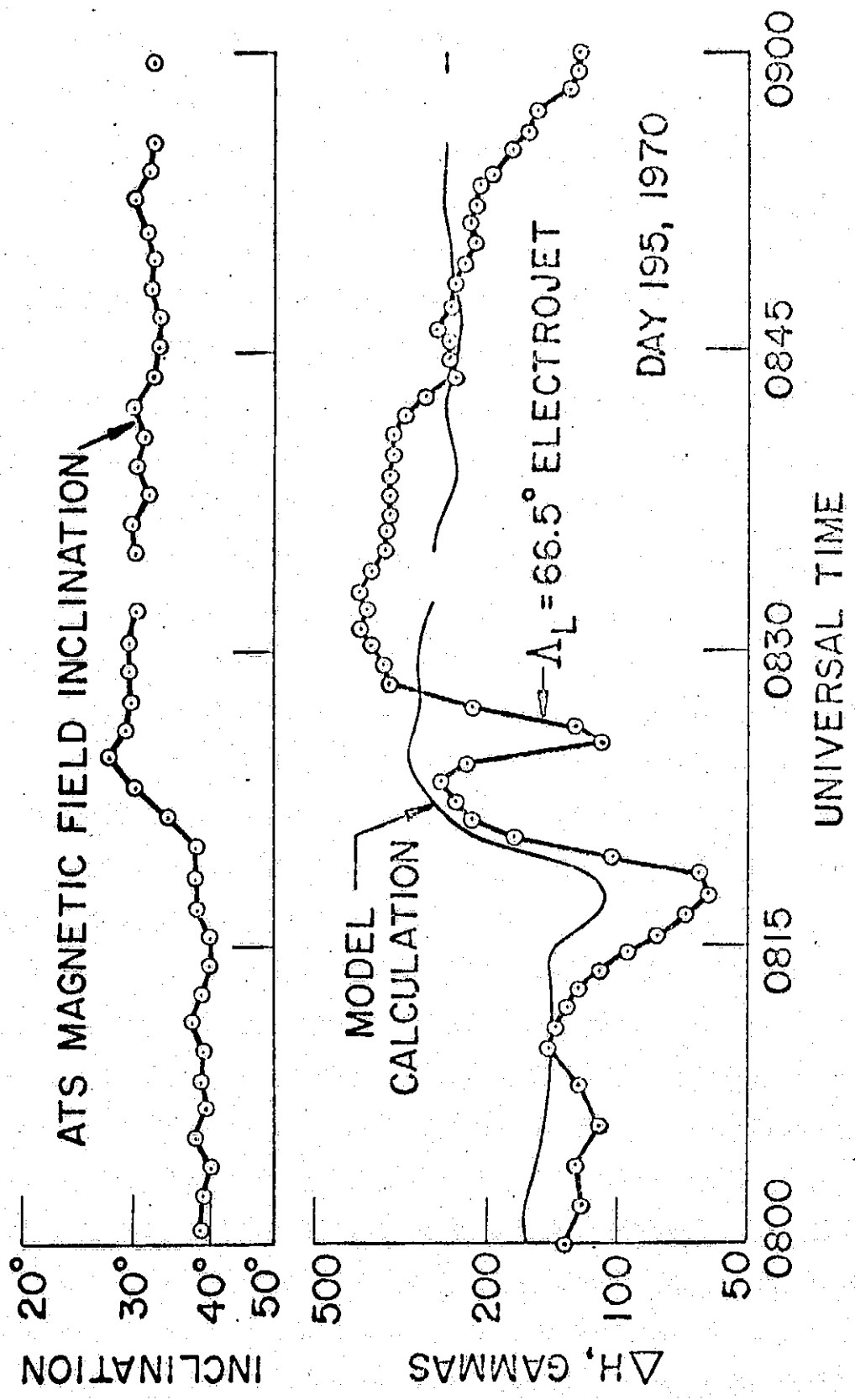


FIGURE 6

N76-15707

A P P E N D I X B

COORDINATED ATS-5 ELECTRON FLUX
AND SIMULTANEOUS AURORAL OBSERVATIONS

S.B. Mende and E.G. Shelley

February 1975

Lockheed Palo Alto Research Laboratory
3251 Hanover Street
Palo Alto, California 94304

ABSTRACT

All Sky Cameras (ASCA) observations were made at the field line conjugate of the ATS-5 Satellite. The field of view of these cameras covered the region of the magnetosphere from $L=5$ to $L=11$ at the approximate longitude of the ATS field line conjugate. With this coverage, definite statements can be made concerning the correlation of the auroras observed by the ASCA's and the magnetospheric trapped fluxes. In general, auroral forms are not simply correlated with the synchronous altitude electron fluxes. The presence of hot plasma at the ATS-5 satellite is a necessary but not sufficient condition for the occurrence of local auroras. On quiet days the hot plasma does not penetrate into the magnetosphere far enough to reach the ATS-5 orbit. Under these conditions no auroras are observed at the field line conjugate, but auroras are usually observed on higher latitude field lines. On more disturbed days, auroral arcs are observed at lower latitudes when the plasma sheet penetrates into the ATS-5 orbit. Significant qualitative correlation between the ASCA data and the trapped fluxes can be observed when a local plasma injection event occurs near ATS-5. The clearest signature of the injection event is magnetic and is most pronounced as a recovery of a negative bay in the north-south component of the field at the ATS-5. The local injection generally produces a break-up event and sometimes a westward traveling surge. However, the most significant correlations are observed with the intensification of the diffuse uniform glow which intensifies during the injection event.

INTRODUCTION

Synchronous altitude satellites offer a unique opportunity to continuously monitor the energetic particles and compare the fluxes with the ground phenomena at the field line conjugate. There have been a number of studies using ground-based measurements and experiments on-board the ATS satellites to investigate the phenomena occurring at the region of the magnetosphere near $L = 6.6$ (Freeman and Maguire, 1967; Lanzerotti et al., 1967; Pfizter and Winkler, 1969; Lezniak and Winkler, 1970; Cummings et al., 1968; DeForest and McIlwain, 1971; McIlwain, 1972).

Individual auroral substorm events were studied by Hones et al. (1971) and Mende et al. (1972). Each of these studies examined an individual substorm using a broad data base including ATS-5 satellite measurements and ground observations in an attempt to understand the specific mechanisms which were responsible for the production of substorms.

Akasofu et al. (1974) addressed the specific question of the relationship between plasma measurements on the ATS-5 satellite and auroral displays near the foot of the ATS-5 field line. This study was based on the ATS-5 plasma detector (UCSD) and the Dominion Observatory all sky cameras operated at Great Whale River. The field of view of the Great Whale River all sky camera does not cover the projected ATS-5 field line conjugate, and this resulted in a fundamental difficulty in drawing detailed conclusions as to whether or not specific local auroral forms were correlated with the synchronous altitude plasma observations.

In this paper we are investigating the correlation of ATS-5 plasma data with all sky camera data taken at Thompson and Gillam, Manitoba. The fields of view from both of these stations cover the projected field line position of the ATS-5, including reasonable dynamic changes in field configuration (see Figure 1). The concentric rings around the station represent the computer generated latitude, longitude loci of the 110 km altitude

points corresponding to zenith viewing angles of 15, 30, 45, 60 and 75°. The computed position of the ATS-5 field line (GSFC 42-66 field model) is also shown on this figure as an elongated rectangle (which allows for the longitudinal drift of the satellite through the period covered by this discussion).

Based on the same field model we have calculated the L value and lines of constant L have been superimposed. Thus, the combined all sky camera field of view from Thompson, Gillam and Fort Churchill include the L value range of 5 to 11. In this field model, the ATS-5 L value is 6.9. The diurnal motion of the field is not expected to be more than about 1° in latitude (Fairfield, 1968). According to Fairfield and Ness (1970), just prior to a substorm onset the field is stretched out toward the tail on the nightside compared to the dipole-like configuration. This results in an estimated additional ATS-5 conjugate point movement of about 1° in latitude. The present investigation of auroras at the conjugate point and particle data at synchronous altitude can be regarded as a search for a method of field line tracing using the auroral particles as tracers. Such data could then be used to test the validity of the field models and would enable us to derive a time dependent model during a substorm. Unfortunately, although good correlations between the auroras observed by the all sky cameras and the trapped synchronous fluxes are found in some cases, the relationship is not unique.

Recently, Sharp et al. (1975) have shown that a quantitative relationship exists between the synchronous altitude particle fluxes and the auroral electrojet current as measured at a ground-based station near the ATS-5 conjugate point during substorms. The explanation of Sharp et al. (1975) relates the electrojet to the trapped fluxes by means of the conductivity enhancement caused by the precipitating fluxes, thus presupposing that there is a definite relationship between precipitating and trapped fluxes. Thus, from their result, one would expect a close correlation between the trapped fluxes measured at ATS-5 and the auroras observed by the ASCA, because the auroras observed by the ASCA are a manifestation of the precipitation.

In order to investigate the correlation between the ATS-5 trapped fluxes and the auroras at the foot of the ATS-5 field line, we have developed a technique for displaying the auroral intensity recorded by the all sky camera film as a function of time for selected locations. The technique involves the optical measurement of the film density at selected points on the all sky camera negative. These points on the film are on north-south lines and their position on the film plate is illustrated in Figure A1 of the Appendix. In this paper we only present the data from points on a north-south line closest to the ATS-5 meridian. Assuming a constant 110 km altitude for the aurora, the geographic position corresponding to these points are shown on Figure 1 by the large dots. In this paper we present ASCA time plots in which the photographic density is plotted as a function of time for these seven points. The ASCA time plot traces are presented in Figure 5, 8, 14, 16 and 18. The traces are ordered with the most northerly location at the top.

If the ATS-5 field line mapped to a fixed location in the ionosphere and the ATS-5 flux measurements were representative of the precipitated flux, then one would expect that one of these traces would be well correlated with the electron energy flux. The method of producing the time plot traces is described in more detail in the Appendix.

ANALYSIS

As a starting point, we will examine the coordinated data available for 2 very quiet days during which the ATS-5 did not encounter significant electron flux enhancements. Since no auroras were observed at the conjugate point during these days, it is reasonable to conclude that the existence of energetic particle fluxes at ATS-5 is a pre-condition for auroras to occur at the field line conjugate.

Then, we will examine two days on which the ATS-5 did encounter significant plasma enhancements as a result of discernible local injection events on the evening-side. In these cases, there is a correlation between the ASCA data and the freshly arrived plasma at the satellite near the line of injection.

Finally, we will examine somewhat more disturbed days on which the plasma enveloped the satellite at fairly early local times and significant auroral activity was observed in the ASCA data. Under these conditions the auroras are generally not well correlated with the drifting plasma clouds, but are correlated only with freshly injected plasma.

QUIET CONDITIONS WITH NO PLASMA INJECTIONS

Figure 2 presents a typical quiet spectrogram from the ATS-5 plasma detector (DeForest and McIlwain, 1971) for day 43, 1970. Day 38 (the spectrogram for day 38 showed even less activity than that for day 43) and 43 were magnetically quiet days and there were no significant electron fluxes observed at ATS-5 during the entire day. The ASCA was operated at Thompson from about 0445 to 0845 UT. A careful study of the all sky camera records for both of these days show no discernible auroral activity at Thompson. The clarity of the sky can be easily established from the all sky camera pictures by means of a star count.

It is interesting to investigate the extent of this aurora free region. All sky camera coverage at Ft. Churchill began at around 0100 UT on day 38. A fairly bright arc appeared around 0450 in a direction somewhat northwest to southeast located near the northern horizon. There was a discernible loop structure on the eastern side, it faded out as it moved southward and disappeared around 0514. A single loop structure appeared on the western horizon at 0612 and an overhead zenith arc intensified. A fairly bright structure persisted on the western horizon around 0648, it intensified and finally appeared as an arc across the northern half of the sky. The night's activity culminated at 0720 when the arc broke up and only patchy structures remained. The sky cleared around 0830 with no additional auroral displays prior to twilight at 1220.

On day 43, the all sky camera at Ft. Churchill was operated from 0049 UT to about 1130 UT. The first discernible auroral display appeared around 0500 UT. It consisted of a zenith arc, slowly intensifying around 0522. It disappeared at 0541 in and reappeared very much more intensely at around 0615. The arc broke up around 0629 forming a loop at

around 0632. The aurora faded out and became very dim around 0650. An arc located somewhat south of the zenith appeared around 0736 showing multiple structure and intensification by 0804. It shifted towards the northern part of the sky and persisted through 0822 and formed a slight loop towards the eastern side of the sky at 0836. A poleward shift took place slowly between 0836 and 0900. Small patchy structures appeared around 0929 near the zenith. Very diffused morning-type auroras were observed around 1107. Auroras remained until twilight, about 1201. However, no auroral displays were observed in the vicinity of the ATS-5 conjugate point.

In summary, both days 38 and 43 showed all the regular features of nightly auroral displays, the southward moving structures, the appearance of overhead features in the early evening hours, the midnight auroral breakup and the patchy diffuse displays following midnight. By comparison with more active days, one would predict that plasma injections were present on the field line above Ft. Churchill and if a satellite similar to ATS-5 could be flown at the L value corresponding to Ft. Churchill, i.e. at a geocentric distance of 8 or 9 earth radius, then one would expect to find plasma clouds at this location.

QUIET CONDITIONS WITH LOCAL PLASMA INJECTIONS

In reviewing the all sky camera and simultaneous ATS-5 data on day 44 (Feb. 13, 1970) (Mende et al., 1972), we found that the first large plasma injection was simultaneous with a substorm occurring around 0530 UT and was associated with an auroral display.

In Figure 3 we present a spectrogram of the UCSD plasma analyzer data for day 44. There are two distinct electron flux intensifications at the satellite. The one already mentioned (0530 UT) and another at around 0720 UT. In Figures 4 we present a collage of the ASCA pictures from Thompson and in Figure 5 the time history plot (Appendix I) of the Thompson data are presented. The first flux intensification which suddenly enveloped the satellite at 0530 correlates very well with the auroral intensification as seen in the time history plots of

Figure 5. This intensification was uniform, extending all the way from the southern-most to the northern-most latitudes.

After this initial substorm there was continued periodic auroral activity. For example, on the northern half of the sky down to the zenith over Thompson there was obvious activity between 0640 and 0710. However, there was no distinctive auroral activity at 0720 and thereafter when the second rapid flux intensification was observed at the satellite. Examining the Thompson all sky camera photographs alone (Figure 4), it would be rather difficult to derive any qualitative difference between the events occurring at 0530 and at 0720. However, following the interpretation of the ATS-5 plasma data by DeForest and McIlwain (1971), the 0530 event was a local injection since the high energy protons trace back to the injection point of 0530. The intensification at 0720 was due to an event which occurred a few minutes prior to the west of the satellite. This can be seen from the slight downward slope of the dispersion trace of the electrons reaching the satellite at this time. Although this event occurred near the satellite, the absence of the protons and the slight slope of the dispersion curve means that this was not truly a local injection event. Thus, the auroras generated simultaneously with the 0530 event resulted from the precipitation of electrons as they were being freshly injected into the region containing the field lines associated with ATS-5. In contrast, the 0720 flux intensification resulted from a drifting plasma cloud in which there was insufficient pitch angle diffusion into the loss cone to maintain auroras which were detectable by the all sky camera.

The difference between the 0530 and 0720 events is also indicated by the behavior of the ATS magnetogram. The first event at 0530 was accompanied by the sudden recovery of the magnetic depression of the B_z (north-south) component of the field at ATS. This was a configuration change (Mende et al., 1971) since the plasma injection should not result in a field recovery; in fact, it should depress the field even further. There was no such magnetic field signature associated with the plasma cloud appearing at 0720; thus, there was no sudden temporal change of the magnetospheric configuration. It should be noted that the ATS-5 was not in an intense flux region prior to

the 0530 event. In fact, it appears that the 0530 injection event covered a broad latitudinal region which included the ATS-5 location.

In Figure 6 we present the day 44 Thompson magnetogram in an expanded time scale. It is noteworthy that the 0720 plasma event does indeed show up quite distinctly in this ground-based magnetogram and in fact is much clearer than in the auroral data. This is consistent with the findings of Sharp et al. (1975).

On February 5, 1970 (Day 36), a single isolated event was observed in the all sky camera data (see Figure 7). Time plots of these ASCA data are presented in Figure 8. These plots illustrate the presence of a southward moving arc starting around 0400 and the sudden appearance of the central arc at around 0432 immediately followed by the breakup and onset. The local time at Thompson during this event was early evening and the direction of the local currents was eastward showing a positive D-component just after 0430. This event is not particularly evident in the H-component at Thompson; however, it does show the commencement of the local activity at about 0430. The positive D-component could be interpreted as an upward moving field aligned Birkeland current north of the station. The H-components from the selected polar stations show a maximum at Churchill at 0430, which is in agreement with the center of the event being poleward of Thompson and outside of ATS-5. A significant field recovery at ATS-5 was observed to coincide with this event.

In Figure 9 we show the Lockheed ATS-5 plasma data. (The plasma properties were derived as per the Appendix of Mende et al., 1972.) We can see that the ATS-5 energy flux climbs very slowly reaching a maximum level at 0500 or later. The electron fluxes observed at the satellite during this event were extremely soft. The event was accompanied by a magnetic reconfiguration signature, at ATS and by a moderate negative bay at Gt. Whale River east of the station, and a strong negative bay at Ft. Churchill north of the station. The sudden positive excursion of the D-component at the local station indicates that the center of the event was possibly poleward from the ATS-5 location. Nevertheless, we would classify this as a local injection event on the basis of field reconfiguration observed by

the ATS-5 magnetometer and it appears that the soft edge of the plasma sheet extended into the region of the ATS-5 satellite (Vasyliunas, 1968; Shelley et al., 1971; Mauk and McIlwain, 1973). This was accompanied by moderate breakup activity at the location of the field line as seen in the all sky camera.

ACTIVE CONDITIONS WITH LOCAL PLASMA INJECTIONS

As the auroral activity increases plasma injection events occur with increasing frequency and the ATS-5 satellite is frequently enveloped by the drifting plasma from earlier injections. On day 326 (1969), a sudden commencement occurred at approximately 0250 UT following a relatively quiet day. Significant magnetic activity continued after the sudden commencement as indicated in the Ft. Churchill magnetogram.

Since the all sky cameras, operated at Thompson and Gillam, were of the rapid run variety, film was conserved by photographing only at times near local midnight. All sky camera data acquisition began at 0451 UT on this day (Fig. 11). Some faint aurora emissions were evident even at this time; however, intense moonlight inhibited very sensitive all sky camera observations. A northern arc intensified at around 0506 and disappeared about 0510. Some multiple overhead arc structure was discernible around 0520. A fairly intense auroral arc appeared near the northern horizon at 0551. The arc was quite disturbed and traveled rapidly southward reaching the zenith by 0555. Another arc, southward of this arc, brightened to about 0557 while the arc at the zenith faded. By 0559, a surge-like loop developed, moved westward, leaving the field of view by 0601. Note that this was a very bright aurora since it was comparable in intensity to the bright moon which was also within the field of view. Additional folds followed the westward motion between 0602 and 0605. At this time a bright arc appeared in the southern half of the sky while the northern portion of the sky was filled with diffused patches of aurora. The arc moved slowly northward reaching the zenith by 0612. The display faded around 0616. There was very little aurora activity discernible in the presence of the bright moonlight following this time.

The auroral event which was observed at about 0600, the most intense up to that time, corresponded closely to the peak in the electron energy flux observed at ATS-5 (Fig. 12). This was probably a local particle injection event since it was accompanied by a recovery of the magnetic field to a more dipole-like configuration as indicated by the ATS magnetogram (Fig. 10) at 0600.

In summary, from the day 326 data taken on November 22, 1969, we can make the following deductions. The ATS entered a region of energetic magnetospheric plasma around 0400-0430. Auroras were present in the sky in the following period, but these auroras were not related in any simple way to the observed plasma at ATS. As has been pointed out (e.g. Akasofu et al., 1974), the auroras are far more dynamic than the trapped particle fluxes observed at synchronous altitude. The only time when auroras were simply correlated with the observed particle fluxes was at times when there was evidence for the injection of fresh particles in the magnetosphere at the location of the satellite associated with magnetic field configuration changes, such as the event observed at approximately 0600.

The night of Nov. 9, 1969 (Day 313) was discussed by Akasofu et al. (1974) based on the Gt. Whale ASCA camera data. This was a very disturbed night with a huge local injection occurring at around 0630. ASCA data was also acquired at Thompson starting at about 0630 UT. Although this was rather late when a large substorm was already in progress, the event is worth investigating in view of the strong correlation between the ATS-5 electrons and the electrojet current throughout the period of several substorms reported by Sharp et al. (1975). The ATS-5 electron, omni-energy flux is shown in Figure 13. The energy flux increased significantly in the period between approximately 0500 and 0730 UT reaching relative maxima at about 0613 and 0730 UT. The all sky camera data are presented as time intensity plots in Figure 14. The ASCA data was essentially saturated between 0630 and 0700 corresponding to hundreds of ergs precipitation (see the omni-energy flux of the trapped particles, Fig. 13). From the ASCA data there is clearly a general decrease in auroral activity by about 0715 UT followed by a reintensification which culminated around 0735-0740. Both of these events are recognizable in the

magnetograms as well as in the ATS trapped fluxes. In particular, the ATS magnetogram indicated a significant recovery to a more dipole-like configuration between 0610 and 0635. Also, at 0730, a small but distinct temporary recovery is observed.

In summary, one observes in these cases that the precipitated fluxes which have a broad spatial extent as observed in the ASCA data are temporally correlated with the trapped particle fluxes as measured at ATS-5. There is evidence from the ATS-5 magnetometer data that all of these events were temporal and that ATS-5 was observing particles which were very recently injected into the inner magnetosphere. During the day 313 event, the broad auroral precipitation was so intense that the entire frame of the ASCA was saturated and individual auroral forms were not discernible if they were present. In contrast, this broad diffused auroral precipitation for the most commonly occurring intensity substorms is near the all sky camera threshold, and can only be brought out by the time plot technique described in the Appendix.

ACTIVE CONDITIONS WITHOUT LOCAL PLASMA INJECTION

From the preceding discussions we have seen that, at least under some conditions, the auroras observed on the field line which maps through the ATS-5 are well correlated with the trapped electron fluxes as observed at ATS-5. In order to complete our study of events in which we have coordinated ASCA and ATS-5 particle data, we will review a typical day (045, 1970) during which both distinct auroras and electron flux intensification events at ATS-5 were observed but for which very poor correlation was found between the two sets of data.

All sky camera observations began at Gillam at 0308 UT (Fig. 15). An auroral arc was present in the field of view north of the station. This arc moved steadily southward until 0350. At 0400, a multiple arc structure appeared which developed into a looped configuration between 0413 and 0425. The most intense structures developed north of the station at 0437. The sky was relatively clear of auroras by 0449 and remained so until 0513. Fresh activity started on the northern horizon at 0523 and an arc began to move southward.

The all sky camera coverage was continued with the Thompson all sky cameras which came on at 0452 (Fig. 17). A southern arc was observed at 0607 which broke up into a rayed north-south aligned formation at 0649. Another pair of arcs intensified at 0706. The northward arc moved equatorward and at around 0730 it became a rayed structure. An intense surge type formation presented itself at 0757 towards the east, but never actually moved westward (Akasofu, 1968). After this relatively eventless period, auroral arcs and patches began to form at 0800 and continued until 0845. The time plots for the Gillam and Thompson ASCA data are shown in Figures 16 and 18 respectively.

The ATS-5 spectrogram of the UCSD plasma detector data for this day (day 45, 1970) is shown in Figure 19 and the electron omni-energy flux derived from the Lockheed data is shown in Figure 20. The electron energy flux began to increase at approximately 0400 UT. This initial flux increase was due to relatively soft electrons (see Figure 19) suggesting the entry of the satellite into the plasma sheet or into a westward drifting plasma cloud. The electron flux continued to increase reaching a small local maximum at about 0430 and began to increase again at about 0450 reaching a broad maximum at about 0540. Other maxima occurred at about 0620 and 0755.

Comparing these times with the times of significant auroral activity near the foot of the ATS-5 field line described above, we find very little detailed correlation between the two sets of data. The time of which the initial rise in electron flux occurred did agree reasonably well with the time at which the auroras first moved southward through the projected location of the ATS-5 field line. Also, the small local maximum in the electron energy flux at about 0430 appears to be associated with the relatively broad enhanced auroral luminosity beginning at about 0430 primarily north of the ATS-5 field line (see Figure 15). It is reasonable to assume that each of the flux intensifications observed at ATS could be traced back to some specific substorm activity at some earlier time by the method of DeForest and McIlwain (1971); however, the purpose of the present study is to investigate the relationship between the instantaneous auroral luminosity and the associated trapped particle

fluxes. From this standpoint we find the correlation throughout this period to be very poor. It should be noted that this is consistent with our observation in the previous events and also those of Sharp et al. (1975) in that the ATS-5 magnetometer did not indicate a local reconfiguration of the tail field and thus these intensifications were not interpreted as local injection events.

In summary, we find that during this active period there was very poor correlation between the synchronous altitude trapped electron fluxes which were not due to local injection events and the corresponding auroral forms observed near the foot of the ATS-5 field line.

CONCLUSIONS

We have inter-compared the trapped electron fluxes at the ATS-5 and the simultaneously measured auroral activity near the projected foot of the ATS-5 field line for several days of varying substorm activity. The comparisons were facilitated by presenting the all sky camera data in the form of time varying luminosity plots. We have found that under certain conditions there was a good correlation between the two sets of data while under other conditions the data sets were poorly correlated.

The ASCA observations of Akasofu et al. (1974) were made at one hour local time east of the calculated ATS-5 field line position. The fact that they observed auroral intensification coincident with plasma injection shows that on a broad scale the auroras are correlated with the magnetospheric ATS-5 (trapped) plasma. We also found that there was good correlation between auroral intensification which took place over a broad latitudinal region and local plasma injection events at ATS-5. It should be noted, however, that part of the diffuse background in the ASCA data may be due to other than direct particle precipitation only. Optical contamination from atmospheric and instrumental scattering from bright auroral features within the ASCA field of view will also produce a general background proportional to the overall auroral activity.

It might also be anticipated that there would be a strong correlation between detailed variations in the trapped flux levels and small scale auroral features or arcs observed near the conjugate point of the flux measurements. The search for such correlating was facilitated by the use of time-intensity plots for the ASCA data. Also, the use of data from multiple ASCA observation sites made it certain that we covered the ATS-5 field line position including reasonable allowance for dynamic variations in position during substorms. We did not find any indication of single auroral features or arcs being correlated with the ATS-5 particle fluxes.

The present results established reasonably well the lack of a detailed correlation between the fine structure of the trapped plasma fluxes and the small scale auroral features. . Such a definitive statement could not be made by Akasofu et al. (1974) because at the one hour local time offset between their particle flux and auroral observations.

The existence of trapped electron fluxes at ATS-5 appears to be a necessary condition for auroral activity in the vicinity of the foot of the field line, but it is not a sufficient condition. The activity associated with the individual auroral forms did not appear to be correlated in any simple way with the variations in the trapped electron fluxes. Furthermore, the variations of the trapped electron fluxes which were interpreted as drifting plasma clouds from previous substorm activity did not necessarily produce increased auroral activity. This suggests that at the time of injection of new plasma into the region of ATS-5 there is significant pitch angle diffusion into the loss cone, consistent with the observations of Sharp et al. (1975). On the otherhand, the pitch angle diffusion within the drifting plasma clouds appears to be much weaker. This is also suggested by the long lifetimes of the plasma clouds (DeForest and McIlwain, 1971).

The failure to discover a detailed correlation between the ATS-5 trapped fluxes and the individual auroral forms suggests that individual forms may be generated at low altitude by some mechanism involving the further energization of particles in the loss cone. Perhaps too much emphasis has been placed on the observation and interpretation of intense visible auroral displays as being important in magnetospheric substorm processes since they may well be the result of low altitude phenomena involving only a fraction of the particles.

ACKNOWLEDGEMENTS

We would like to express our thanks to Dr. R.C. Gunton of Lockheed Palo Alto Research Laboratories who set up the Thompson all sky camera stations in late 1969. We are grateful to Dr. R.H. Fether of Boston College for the Gillam ASCA photography coverage and his helpful comments on this paper. Prof. C.E. McIlwain and Dr. Sherman DeForest of the University of California-San Diego have provided the UCSD plasma spectrograms. We gratefully acknowledge their permission to present their data. Thanks are due to the Dominion Observatory for the operation of the all sky cameras at Ft. Churchill and the magnetometer at Lynn Lake and Thompson.

Part of this work was supported by NASA under contracts NASw-2552 and NASw-2656 and part by the Lockheed Independent Research Programs.

APPENDIX I

The Digitization of All Sky Camera Pictures

In order to facilitate the comparison of all sky camera pictures with other forms of time series data it was felt desirable to generate a time history plot from the ASCA data. The advantages of this type of presentation which complement the conventional photographic presentation are self-evident.

In this technique, the all sky camera frames were illuminated by a uniform light source. A TV camera using a silicon vidicon was used to view the frame under examination. The video signal generated by this camera was digitized 256 samples per TV line for 10 selected TV lines per frame and was written in a digital form on an incremental tape recorder. Calibration reference frames were also recorded with zero transmission through the frame and with known transmission. These reference frames were used for calculating the percentage transmission of the all sky camera picture at appropriate points. The ten equally spaced lines were digitized with 6-bit resolution (64 level grey-scale quantization). The lines were in the north-south direction. Seven points on each line were selected for the time history plots.

A computer generated plot of a digitized all sky camera frame is shown on Figure A1. The curves represent the 256 intensity points taken along each line. The small circles represent the positions of the points which were selected for time history plots. Actually, four adjacent samples were averaged for each of the selected points.

In the presentation of the time history plots, such as Figures 5, 8, 14, 16 and 18, the average intensities for the seven selected points are plotted, one above the other. The time plot nearest to the bottom represents

the most (south) equatorward point on the frame and the time plot nearest to the top represents the most (north) poleward point. The generation of these time history plots make it possible to directly compare the ASCA data with other time varying phenomena such as the particle fluxes and magnetograms and thus make more definitive statements about their correlations.

REFERENCES

- Akasofu, S.I., S. DeForest and C. McIlwain; "Auroral displays near the foot of the field line of the ATS-5 satellite," *Planet.Space Sci.* 22, 25, 1974.
- Akasofu, S.I.; Polar and Magnetospheric Substorms, p. 27, Springer, New York, 1968.
- Akasofu, S.I. and C.I. Meng; "A study of polar magnetic substorms," *J. Geophys. Res.* 74, 293, 1969.
- Cummings, W.D., Barfield, J.N. and Coleman, P.J., Jr.; "Magnetospheric substorms observed at the synchronous orbit," *J. Geophys. Res.* 73, 6687, 1968.
- DeForest, S.E. and McIlwain, C.E.; "Plasma clouds in the magnetosphere," *J. Geophys. Res.* 76, 3587, 1971.
- Fairfield, D.H.; "Average magnetic field configuration of the outer magnetosphere," *J. Geophys. Res.* 73, 7329, 1968.
- Fairfield, D.H. and N.F. Ness; "Configuration of the geomagnetic tail during substorms," *J. Geophys. Res.* 75, 7032, 1970.
- Freeman, J.W., Jr. and Maguire, J.J.; "Gross local time particle asymmetries at the synchronous orbit altitude," *J. Geophys. Res.* 72, 5257, 1967.
- Hones, E.W., Jr., R.H. Karas, L.J. Lanzerotti and S.I. Akasofu; "Magnetospheric substorms on 14 September 1968," *J. Geophys. Res.* 76, 6765, 1971.
- Lanzerotti, L.J., C.S. Roberts and W.L. Brown; "Temporal variations in the electron flux at synchronous altitudes," *J. Geophys. Res.* 72, 1967, 1967.
- Lezniak, T.W. and J.R. Winckler; "Experimental study of magnetospheric motions and the acceleration of energetic electrons during substorms," *J. Geophys. Res.* 75, 7075, 1970.
- Mauk, B.H. and C.E. McIlwain; "Substorm plasma boundaries and Kp," Presented at the Chapman Memorial Symp. on Magnetospheric Motions, 18-22 June 1973, Boulder, Colo.
- Mende, S.B., R.D. Sharp, E.G. Shelley, G. Haerendel and E.W. Hones, Jr.; "Coordinated observations of the magnetosphere: The development of a substorm," *J. Geophys. Res.* 77, 4682, 1972.

McIlwain, C.E.; "Plasma convection in the vicinity of the geosynchronous orbit," Earth's Magnetospheric Processes (Ed. B.M. McCormac). Reidel, Dordrecht, Holland.

Pfitzer, K.A. and J.R. Winckler; "Intensity correlations and substorm electron drift effects in the outer radiation belt measured with the OGO-3 and ATS-1 satellites," J. Geophys. Res. 74, 5005, 1969.

Sharp, R.D., E.G. Shelley and G. Rostoker; "A relationship between synchronous altitude electron fluxes and the auroral electrojet," J. Geophys. Res., June 1975 (in press).

Shelley, E.G., R.G. Johnson and R.D. Sharp; " Plasma sheet convection velocities inferred from electron flux measurements of synchronous altitude," Radio Science 6, 305, 1971.

Vasyliunas, V.M.; "A survey of low-energy electrons in the evening sector of the magnetosphere with OGO 1 and OGO 3," J. Geophys. Res. 73, 2839, 1968.

LIST OF FIGURES

- Figure 1 Computer-generated map of all sky camera field of views at Ft. Churchill, Gillam, Thompson and Gt. Whale River. The curves surrounding the stations represent field of view angles from 15° , 30° , 45° , 60° and 75° for a 110 km assumed altitude. From the GSFC 12-66 field model the invariant L values were computed and superimposed. Using the same model, the approximate position of the field line intersect is shown as a small rectangle. The solid dots represent the geographic positions of the ASCA time plot traces from the Thomson ASCA.
- Figure 2 UCSD spectrogram for ATS-5 for day 43 (Feb. 12, 1970).
- Figure 3 UCSD spectrogram for ATS-5 for day 44 (Feb. 13, 1970).
- Figure 4 ASCA pictures, Thompson, Feb. 13, 1970.
- Figure 5 ASCA time plot, Thompson, Feb. 13, 1970. The seven traces represent the seven locations shown on Fig. 1 by the large dots. Top trace corresponds to northward point.
- Figure 6 Thompson magnetometer H-component, Feb. 13, 1970.
- Figure 7 ASCA pictures, Gillam, Feb. 5, 1970.
- Figure 8 ASCA time plot, Gillam, Feb. 5, 1970.
- Figure 9 Lockheed ATS-5 particle data.
- Figure 10 Magnetometer H-component data, Nov. 22, 1969.
- Figure 11 ASCA pictures, Thompson, Nov. 22, 1969.
- Figure 12 Lockheed ATS-5 particle data, Nov. 22, 1969.
- Figure 13 Lockheed particle data, ATS-5, Nov. 9, 1969.
- Figure 14 ASCA time plot, Thompson, Nov. 9, 1969.
- Figure 15 ASCA pictures, Gillam, Feb. 14, 1970.

- Figure 16 ASCA time plot, Gillam, Feb. 14, 1970.
- Figure 17 ASCA pictures, Thompson, Feb. 14, 1970.
- Figure 18 ASCA time plot, Thompson, Feb. 14, 1970.
- Figure 19 UCSD plasma experiment, ATS-5.
- Figure 20 Lockheed particle data for Feb. 14, 1970.
- Figure A1 Computer presentation of single frame as digitized with the system. Ten TV lines north-south aligned are digitized in 256 samples each. The circles represent positions from which time history plot curves are produced.

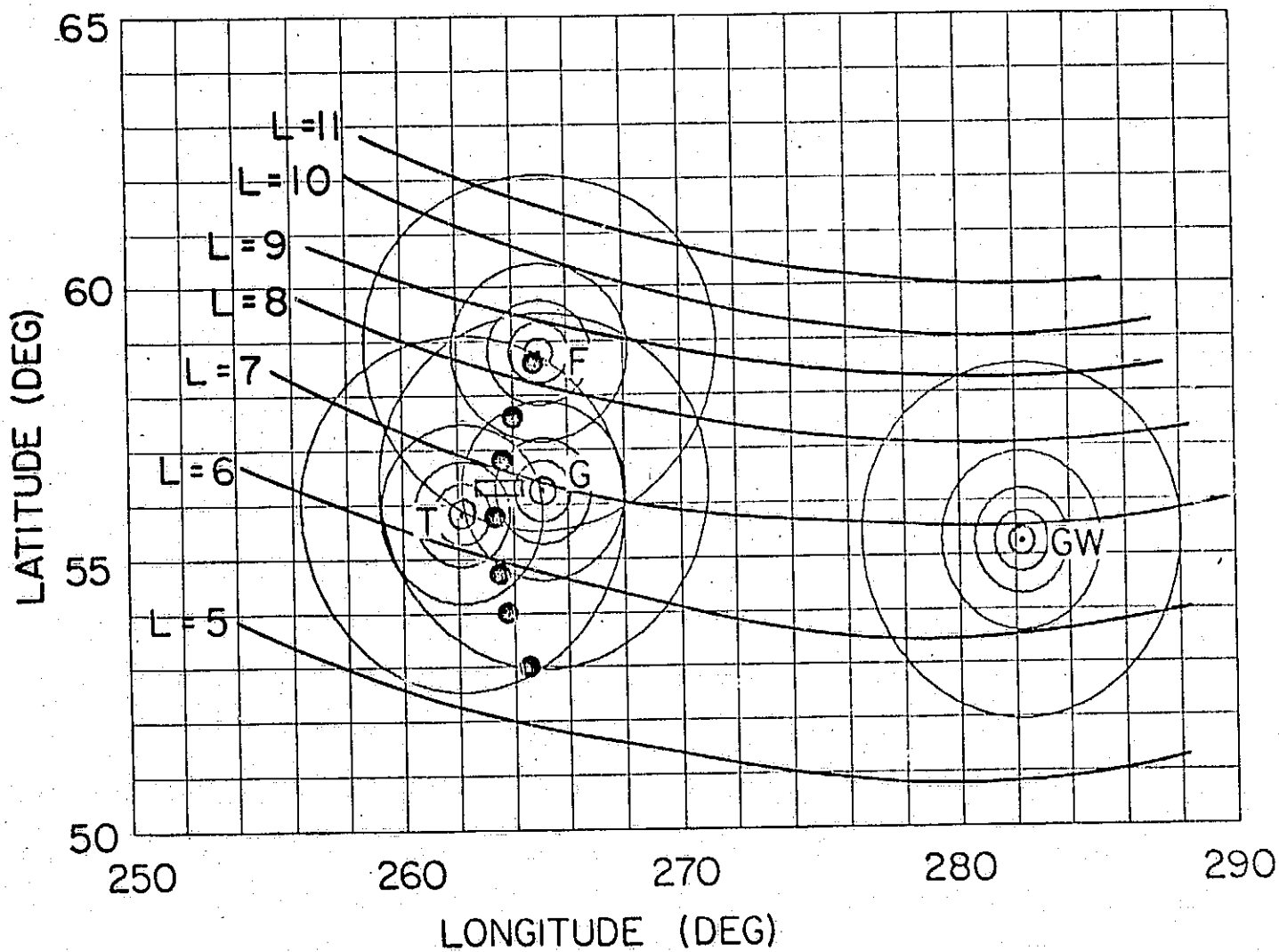
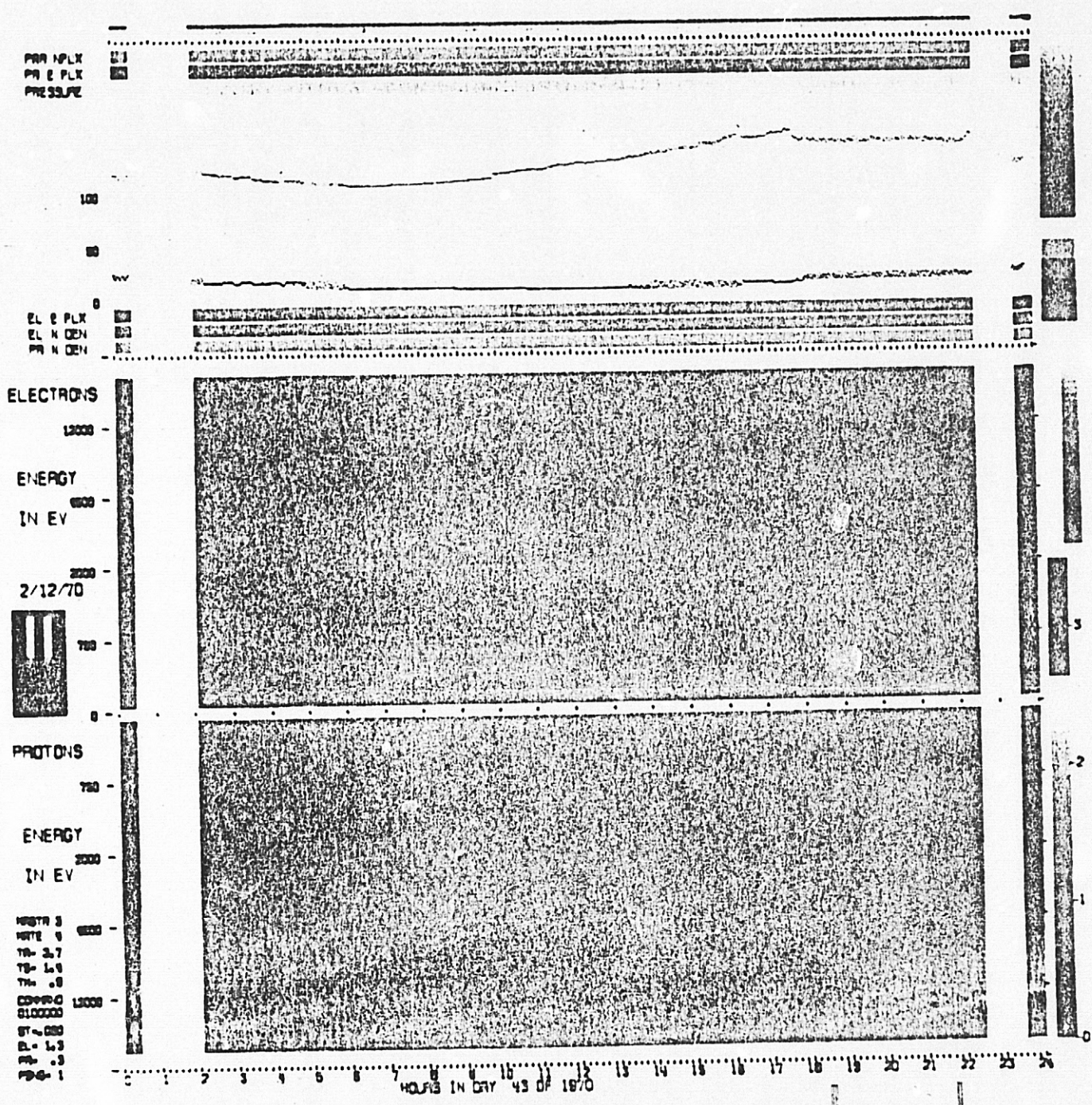


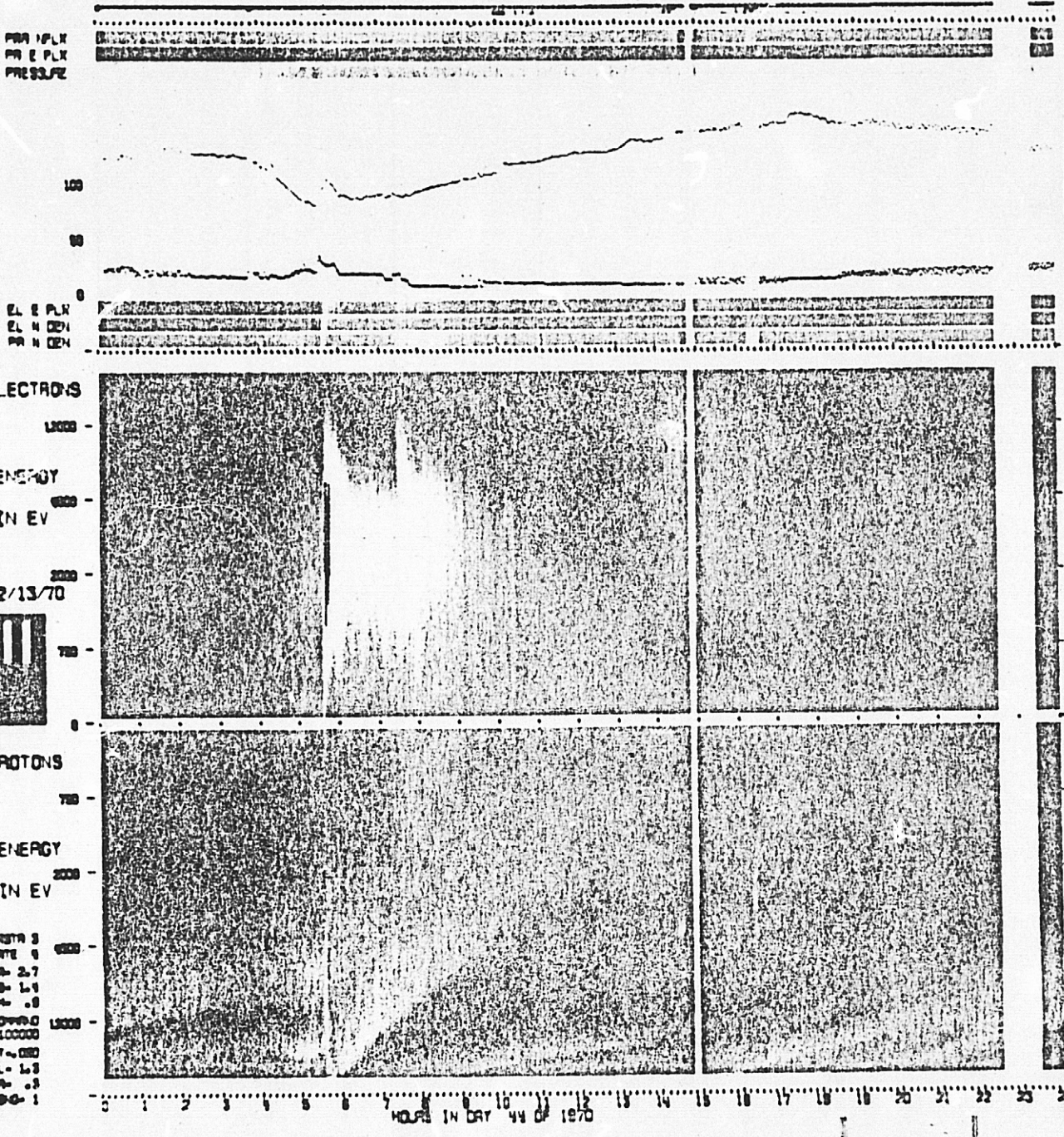
Figure 1

PRECEDING PAGE BLANK NOT FILMED



ORIGINAL PAGE IS
 OF POOR QUALITY

Figure 2



ORIGINAL PAGE IS
 OF POOR QUALITY

Figure 3

THOMPSON, ASCA TIME PLOT, DAY 44, 1970

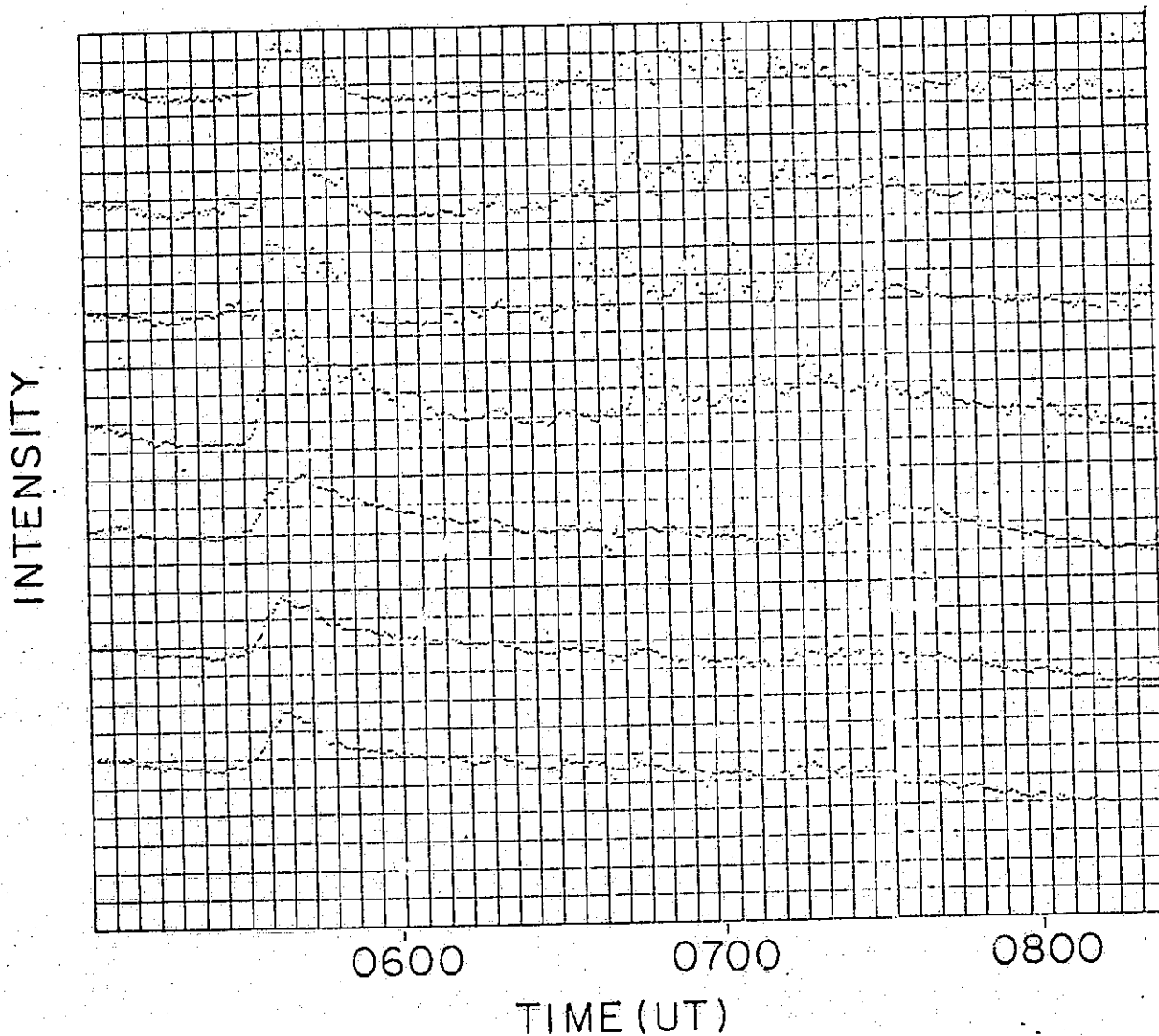


Figure 5

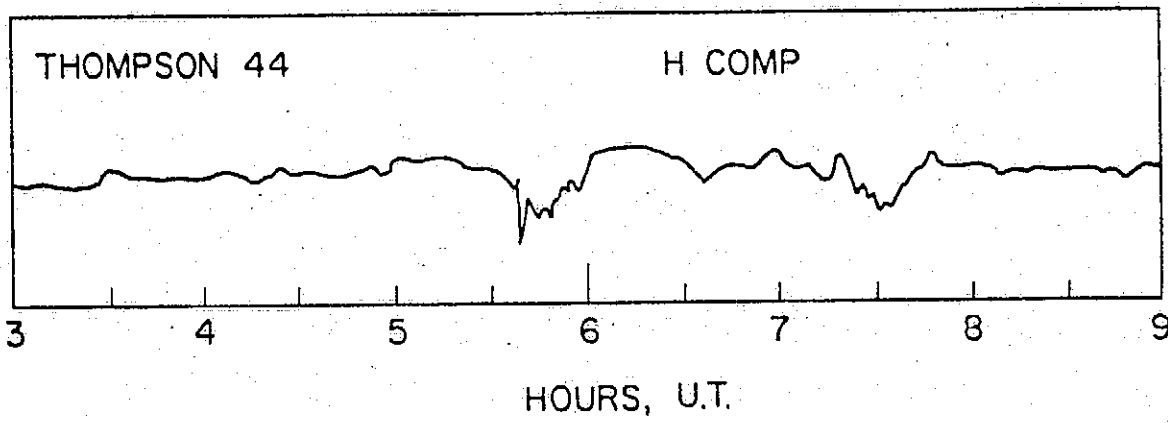
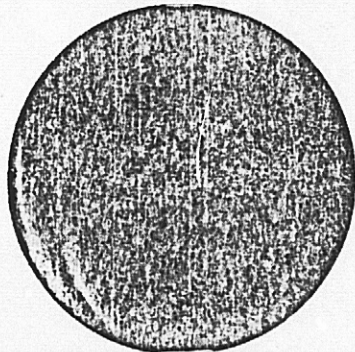
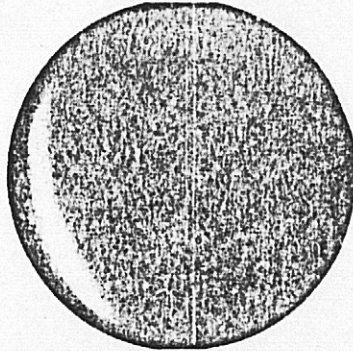


Figure 6

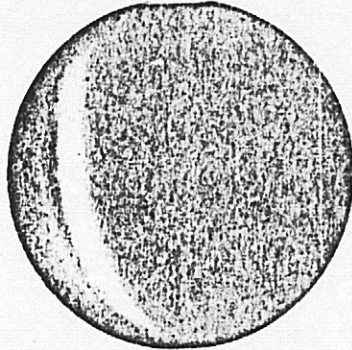
DAY 36, 1970



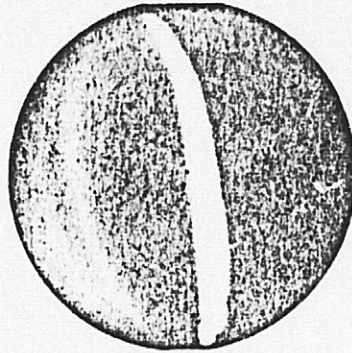
0254



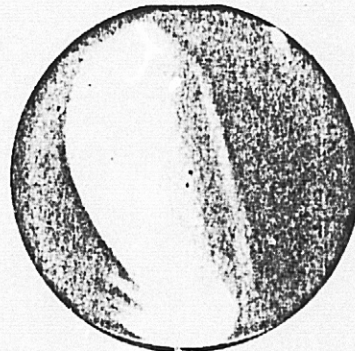
0412



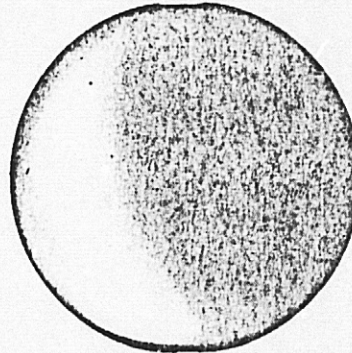
0427



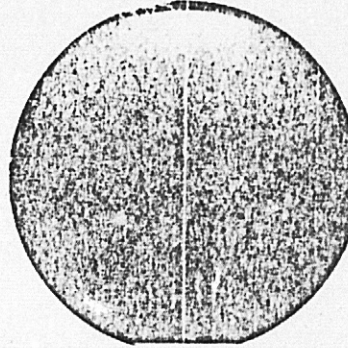
0432



0435



0438

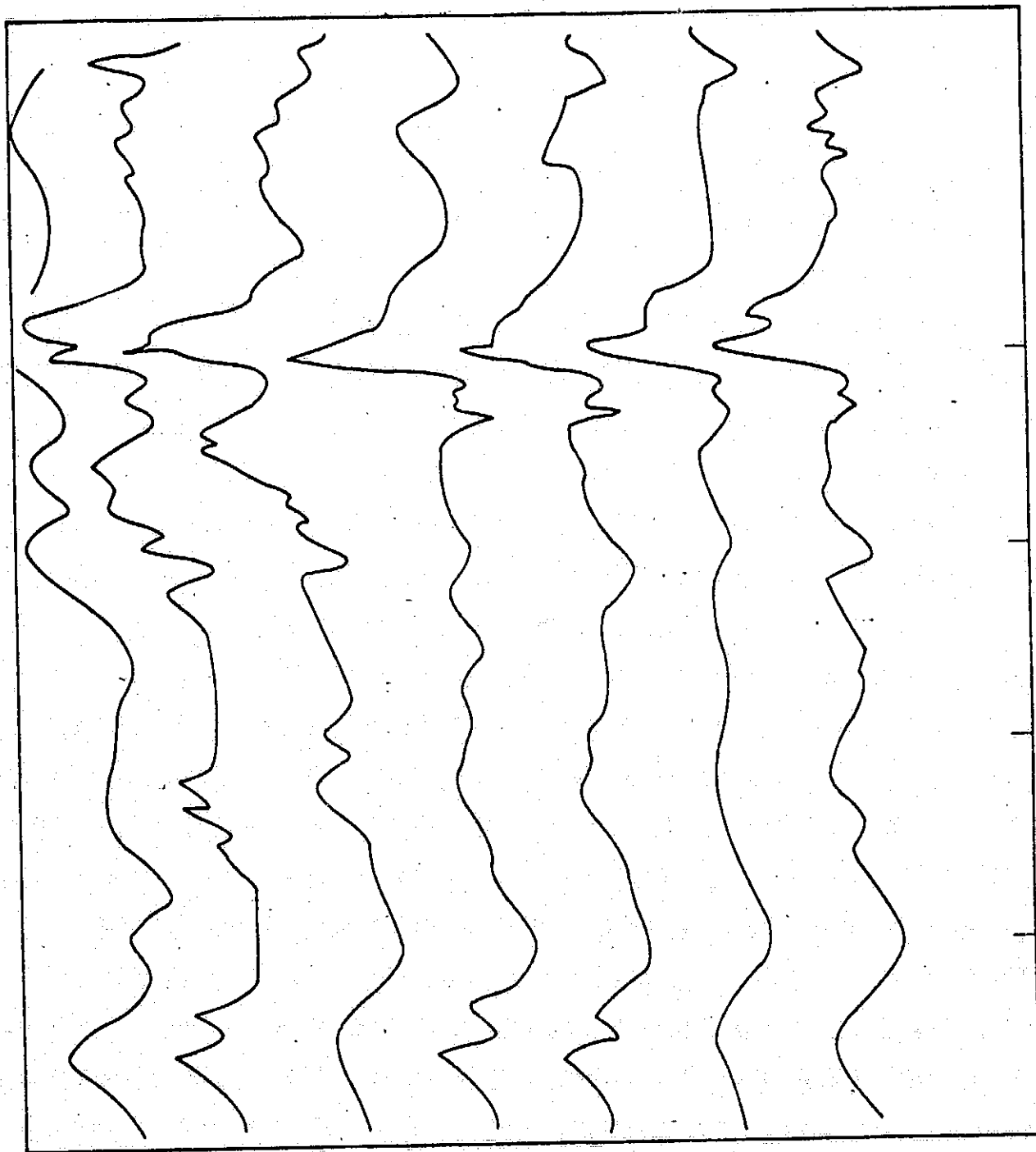


0510

ORIGINAL PAGE IS
OF POOR QUALITY

Figure 7

GILLAM, ASCA TIME PLOT, DAY 36, 1970



U.T. 0230 0300 0330 0400 0430

Figure 8

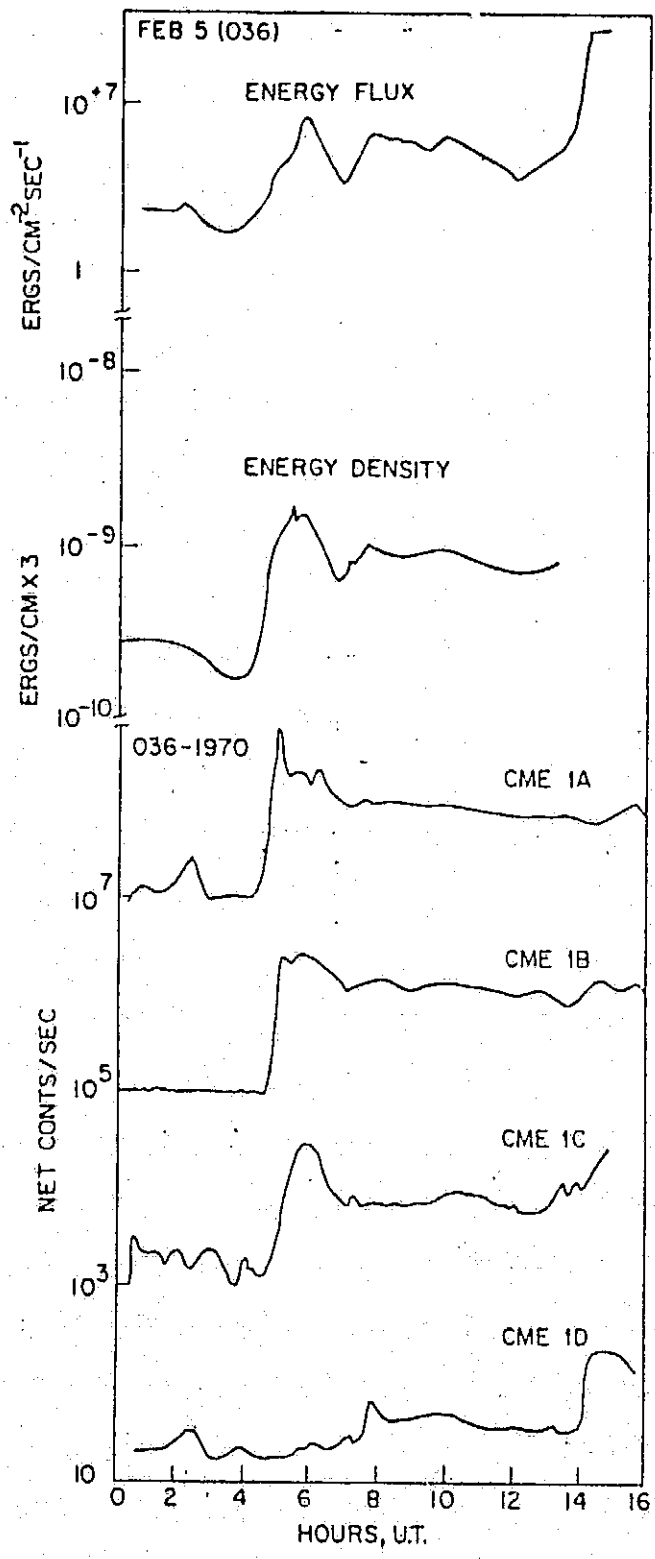


Figure 9

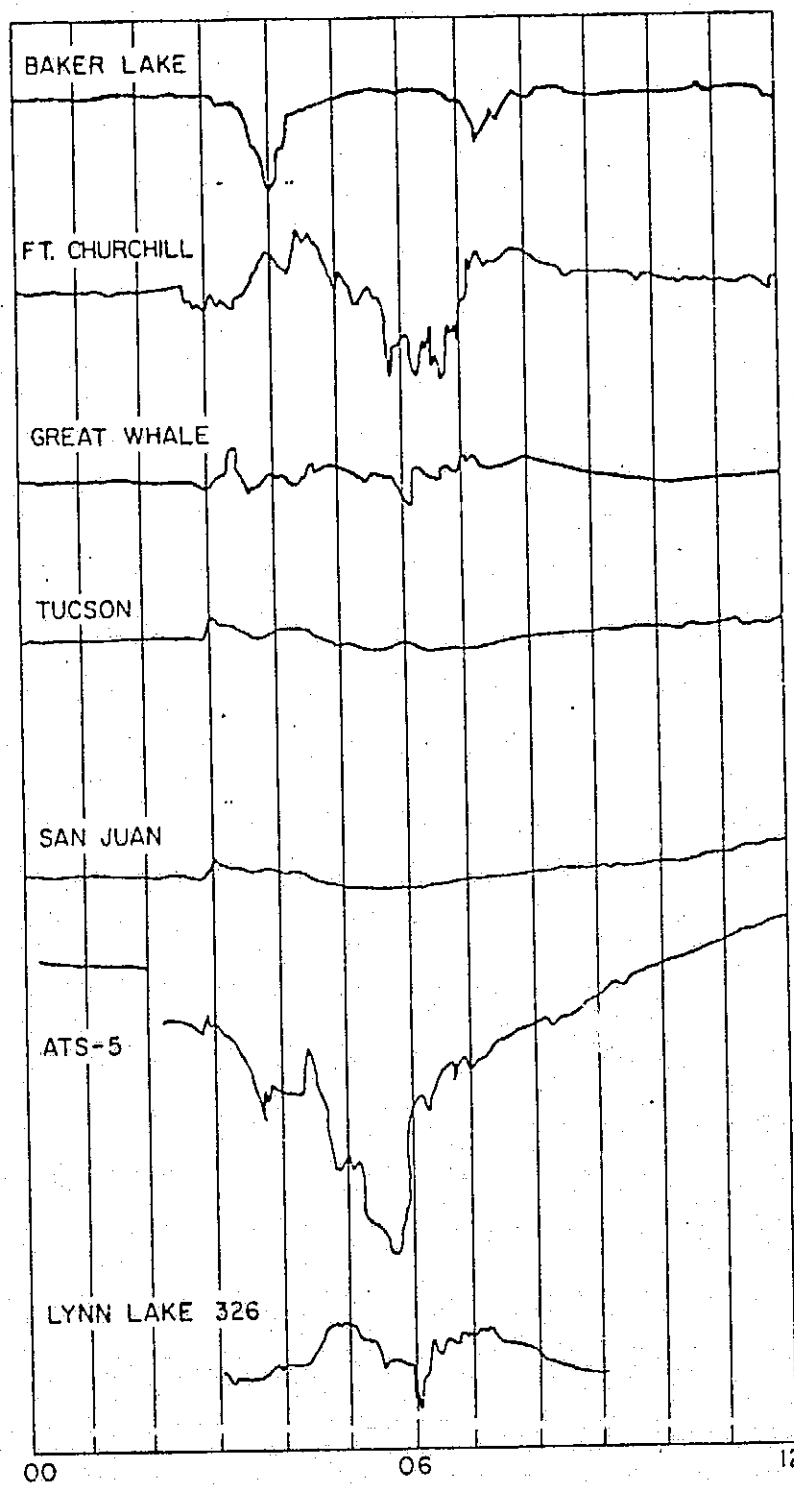
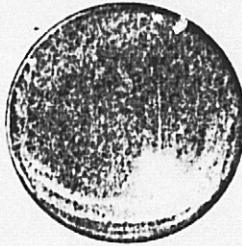


Figure 10

DAY 326, 1969



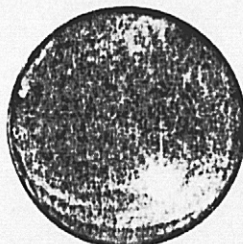
0554



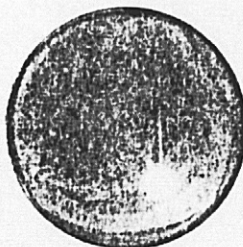
0556



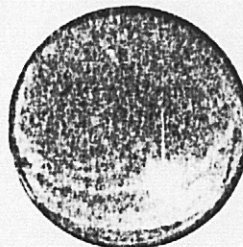
0558



0559



0600



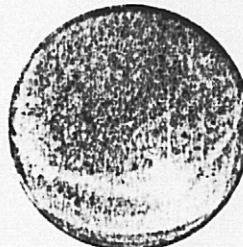
0602



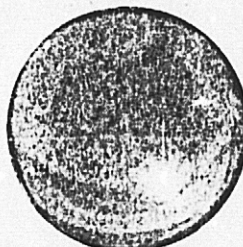
0603



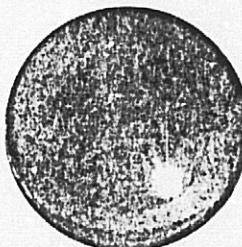
0605



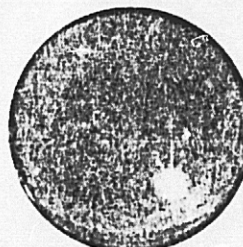
0606



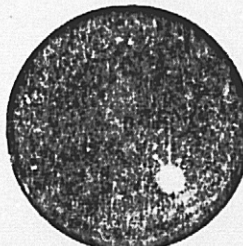
0607



0609



0611



0614

**ORIGINAL PAGE IS
OF POOR QUALITY**

Figure 11

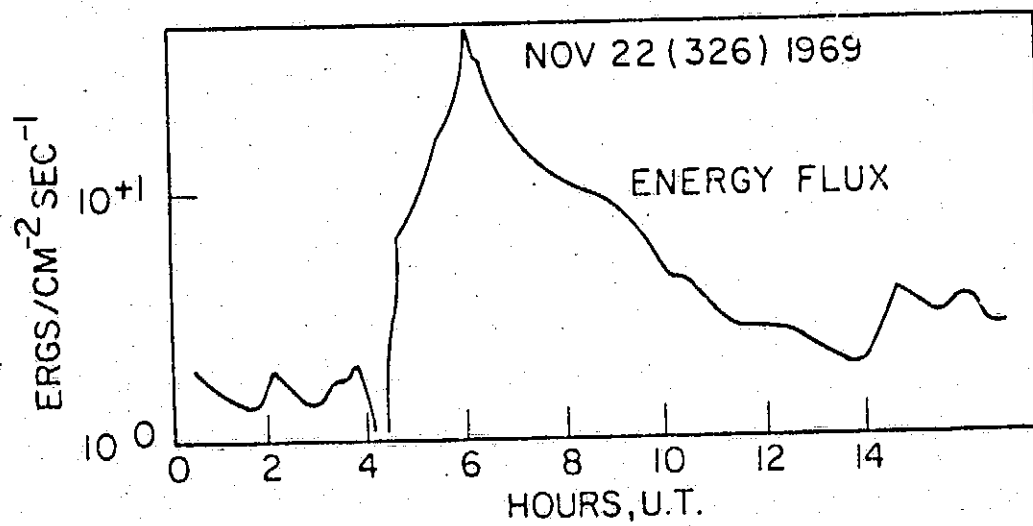


Figure 12

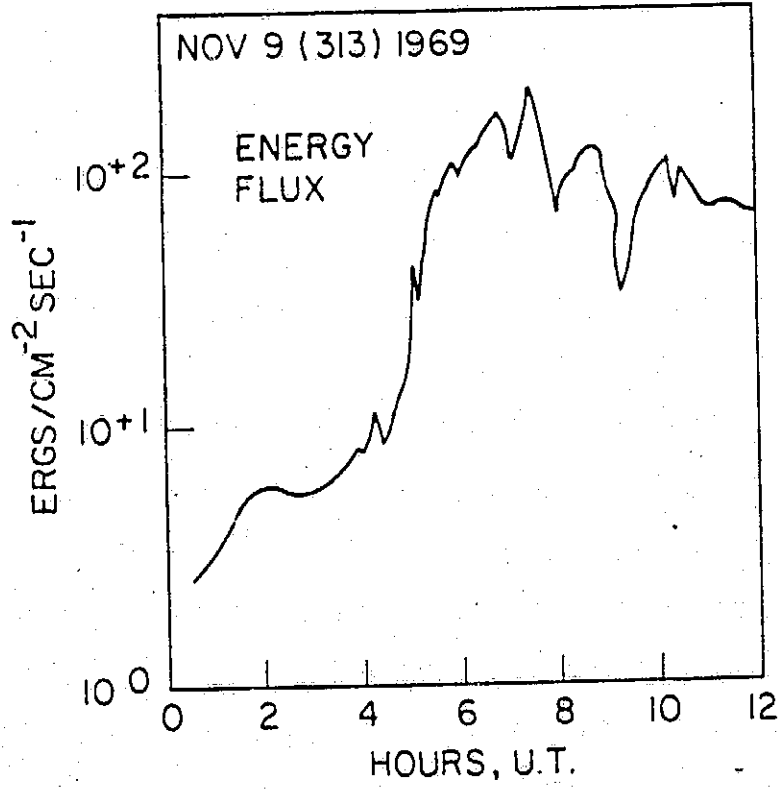


Figure 13

THOMPSON, ASCA TIME PLOT, DAY 313, 1969

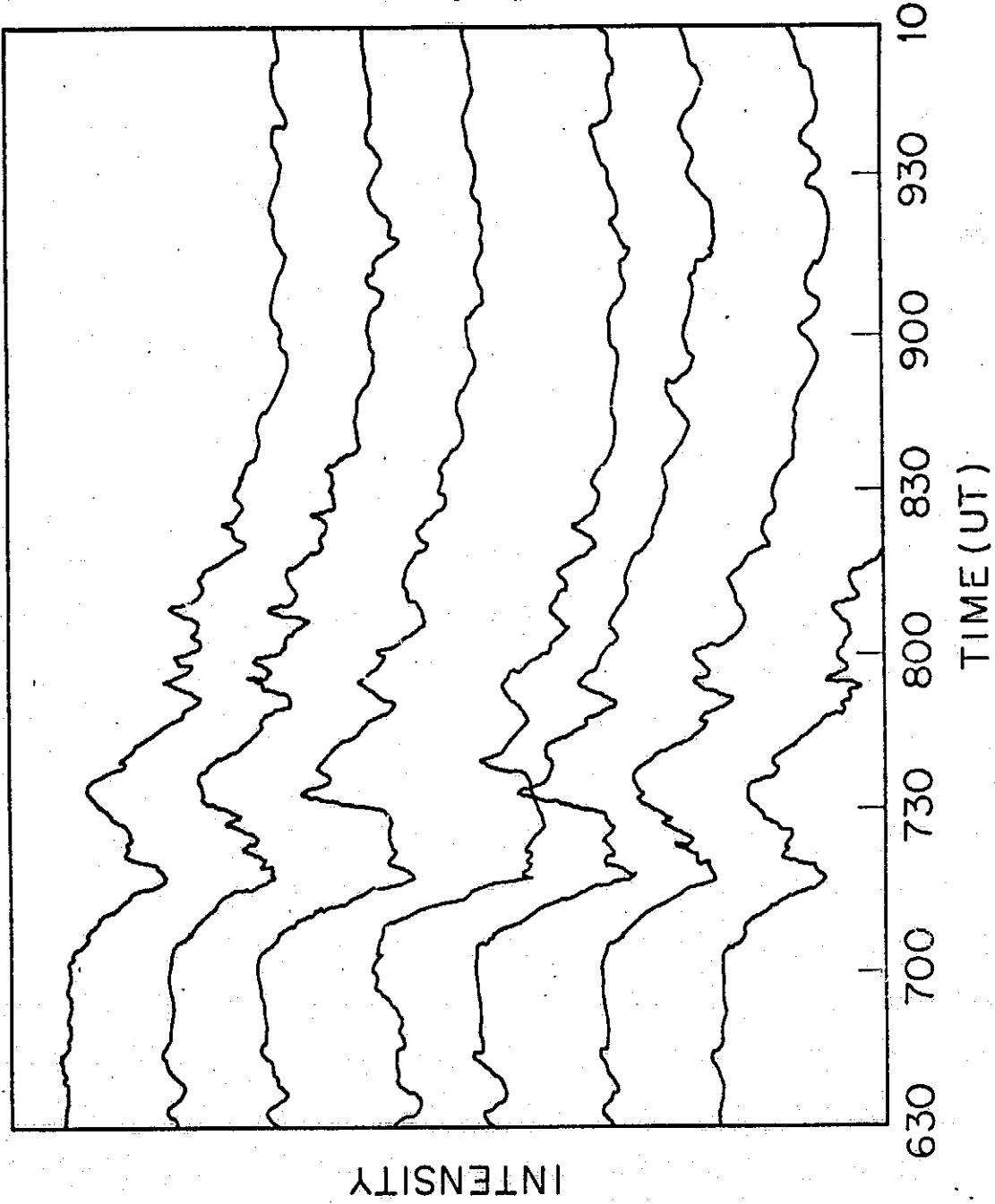
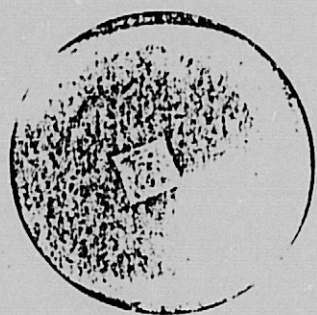
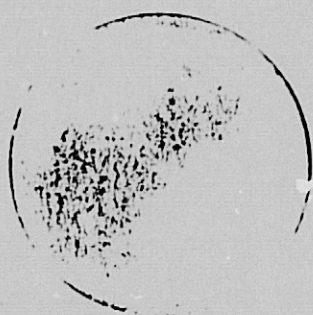


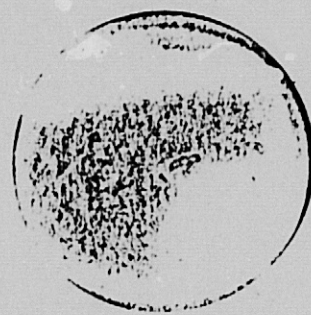
Figure 14



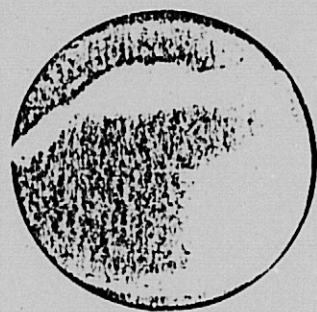
0308



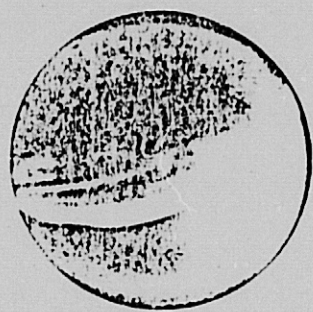
0313



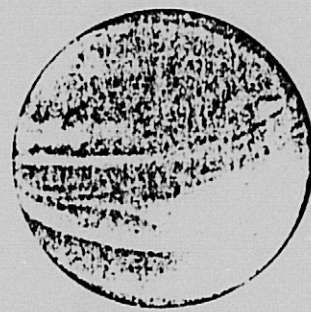
0325



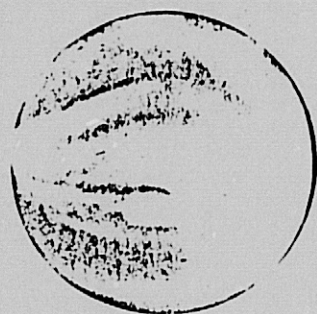
0338



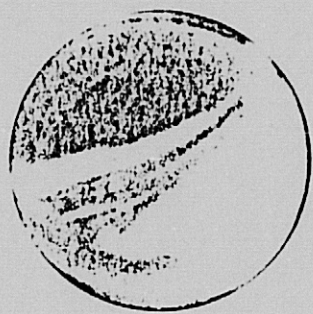
0350



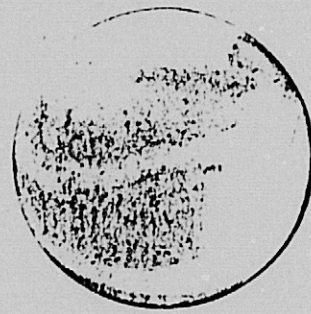
0400



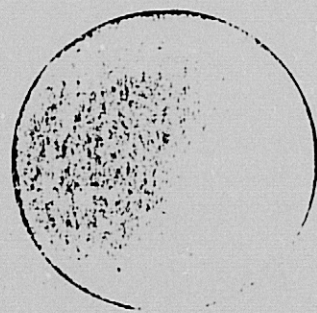
0413



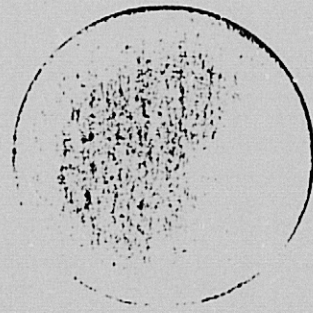
0425



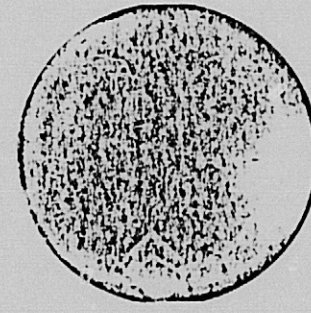
0437



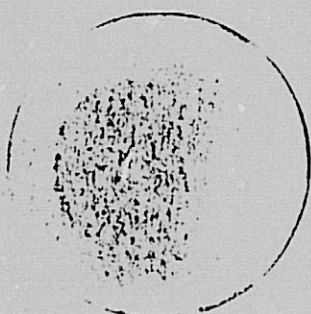
0449



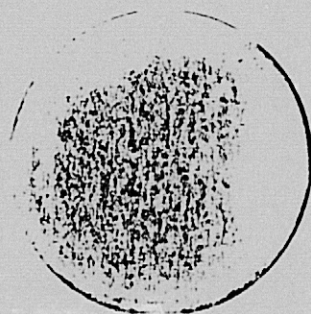
0500



0513



0523



0536

ORIGINAL PAGE IS
OF POOR QUALITY

Figure 15

GILLAM, ASCA TIME PLOT, DAY 45, 1970

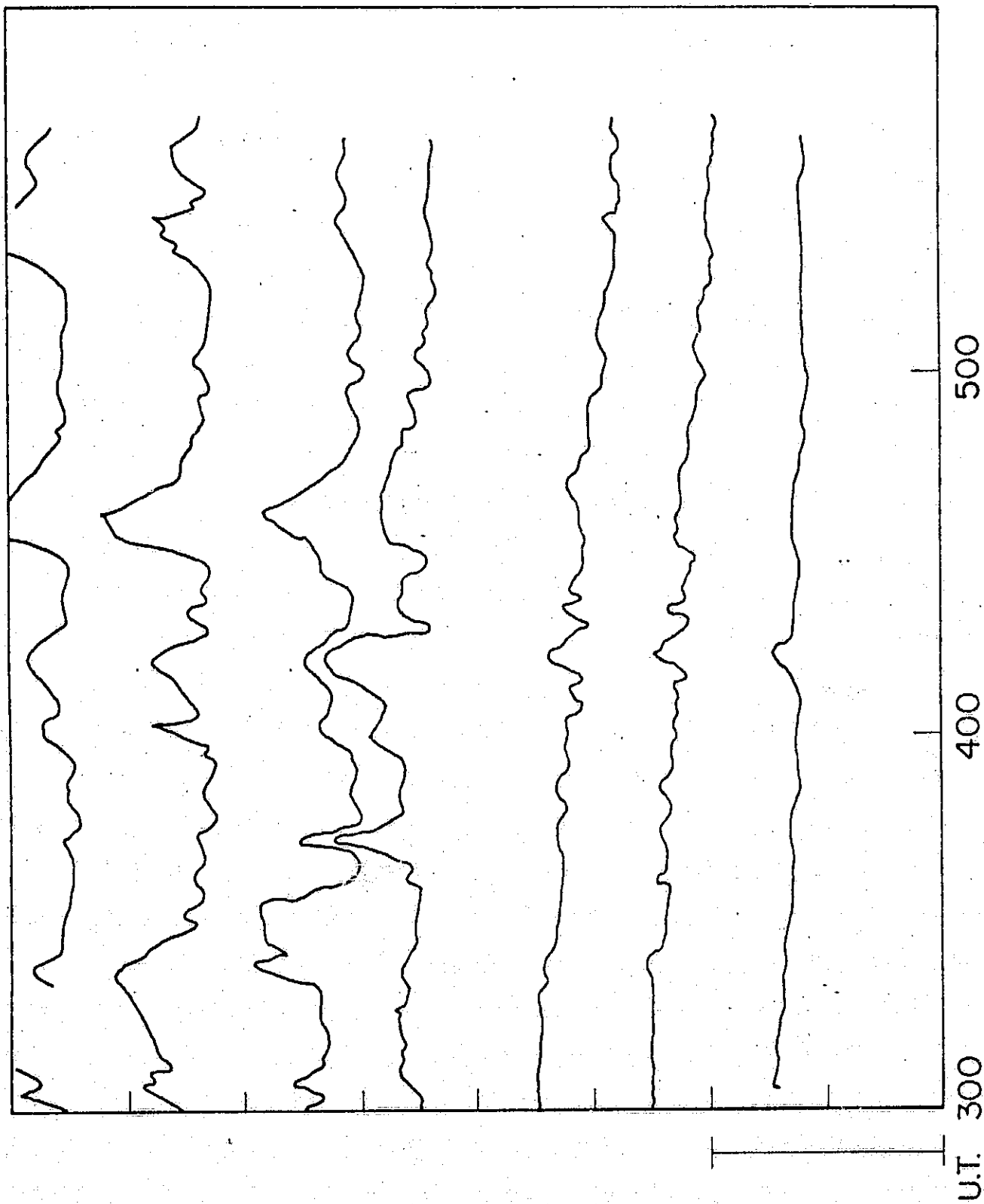
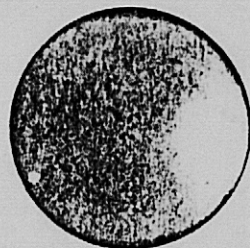
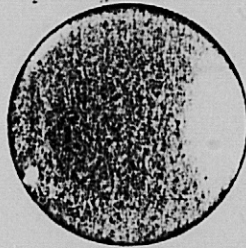


Figure 16

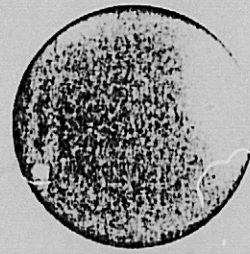
DAY 45, 1970



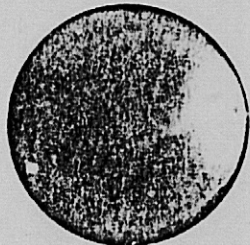
0452



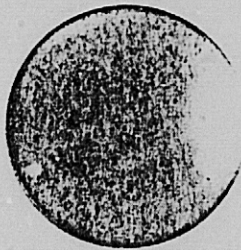
0546



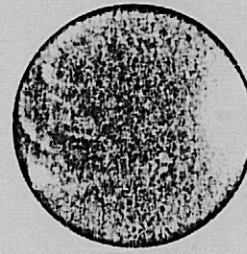
0550



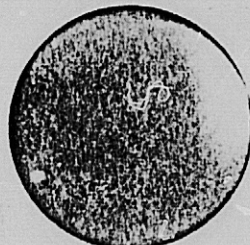
0555



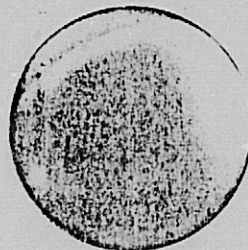
0607



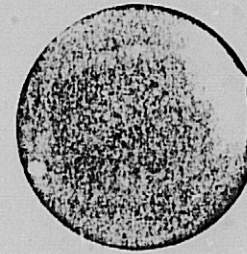
0649



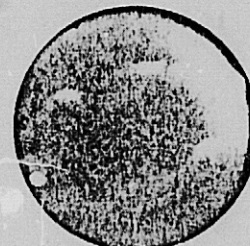
0702



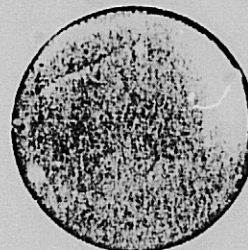
0706



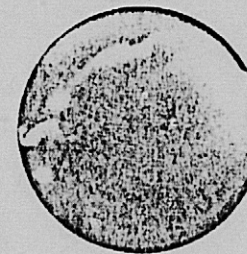
0726



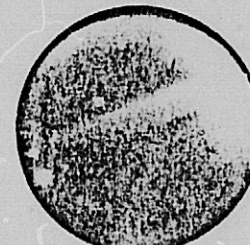
0730



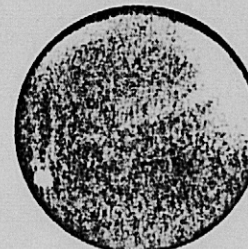
0754



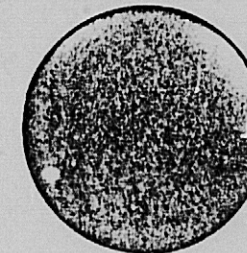
0757



0810



0814



0845

Figure 17

ORIGINAL PAGE IS
OF POOR QUALITY

DAY 045, 1970, THOMPSON

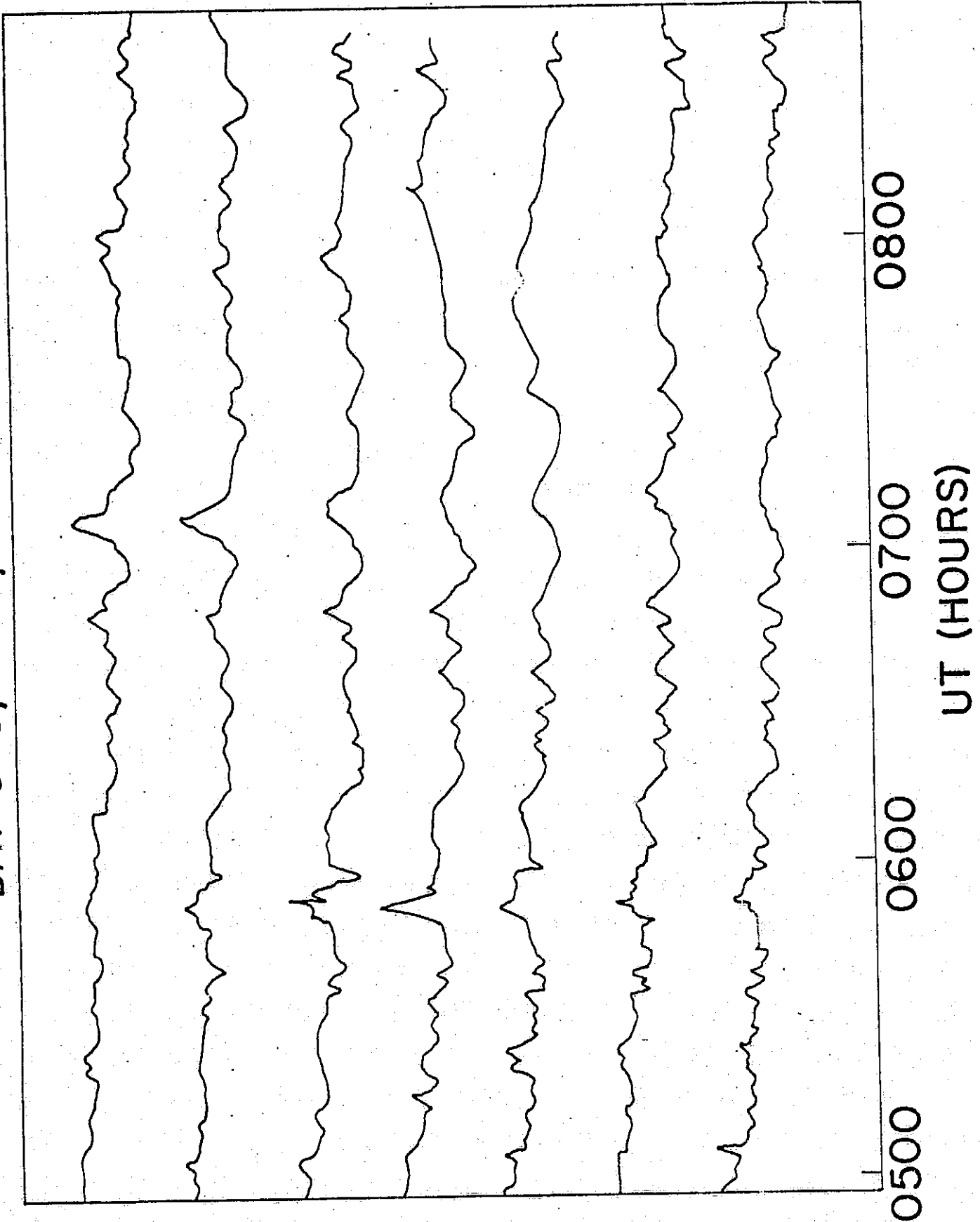


Figure 18

PAR PLX
EL E PLX
PRESSURE

100

50

0

EL E PLX
EL N DEN
PR N DEN

ELECTRONS

12000

ENERGY

IN EV

2000

2/14/70

750

0

PROTONS

750

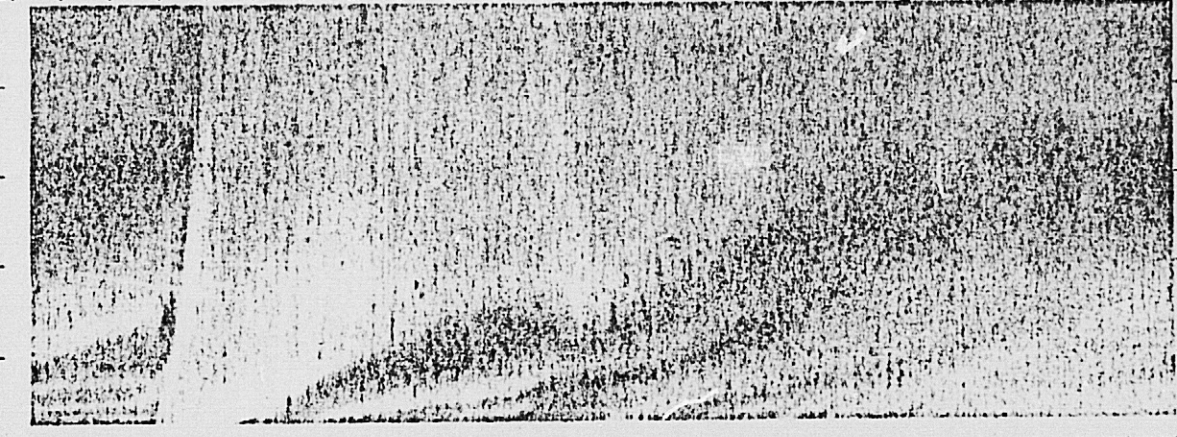
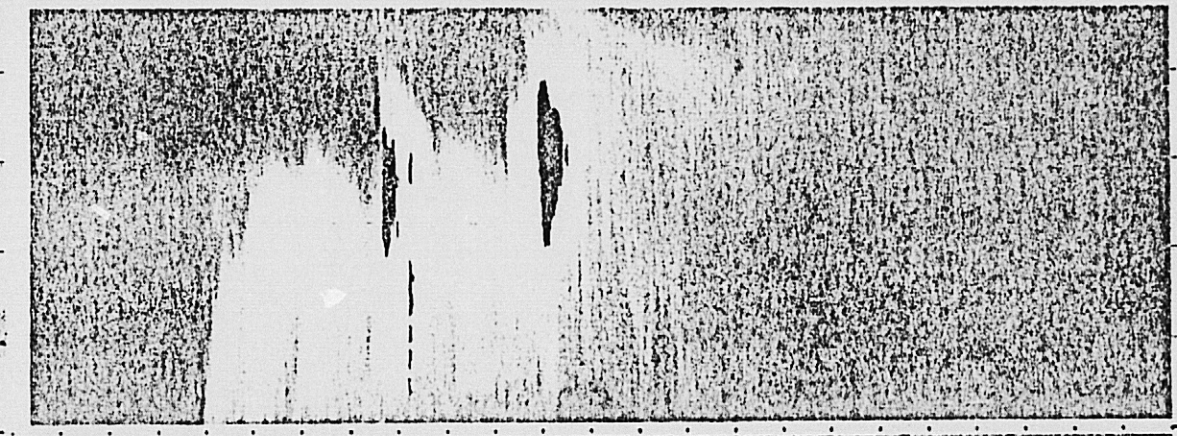
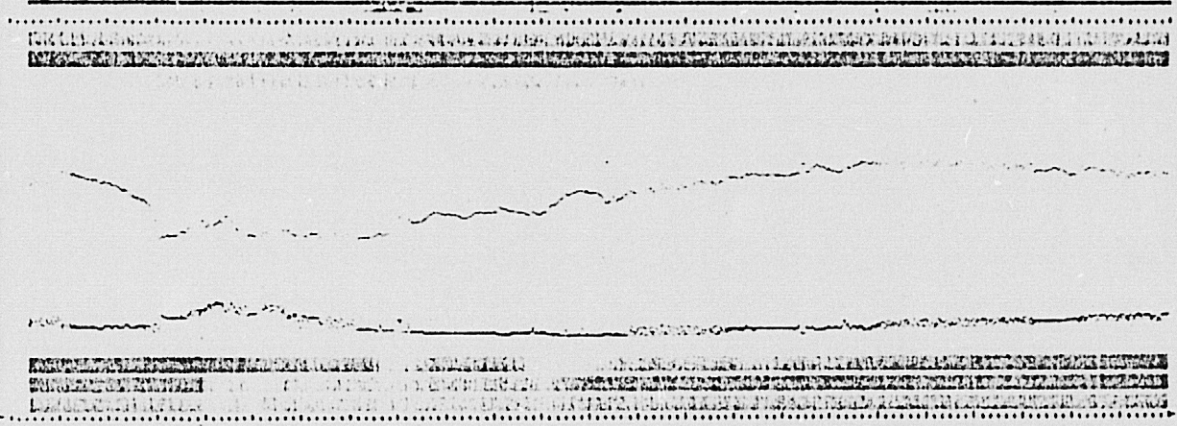
ENERGY

IN EV

2000

12000

MSTR 1
MTE 1
TA- 2.7
TS- 1.9
TN- .9
COMPO 0
0100000
ST- 080
EL- 1.3
PR- .3
794-1



HOURS IN DAY 45 OF 1970

Figure 19

ORIGINAL PAGE IS
OF POOR QUALITY

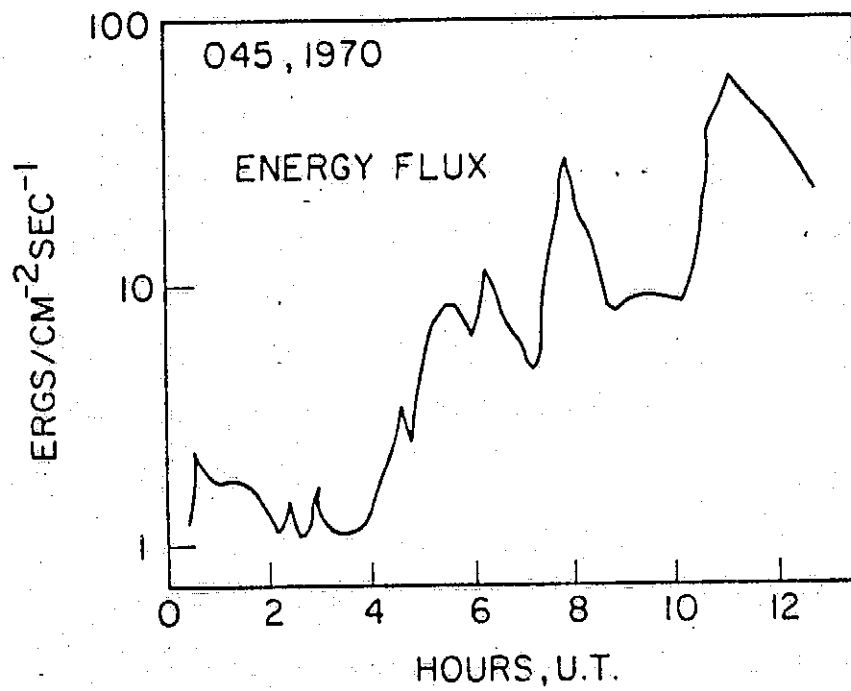


Figure 20

THOMPSON, ASCA PLOT, DAY 44, 1970
AW

U1108/SC4020
0000 0002

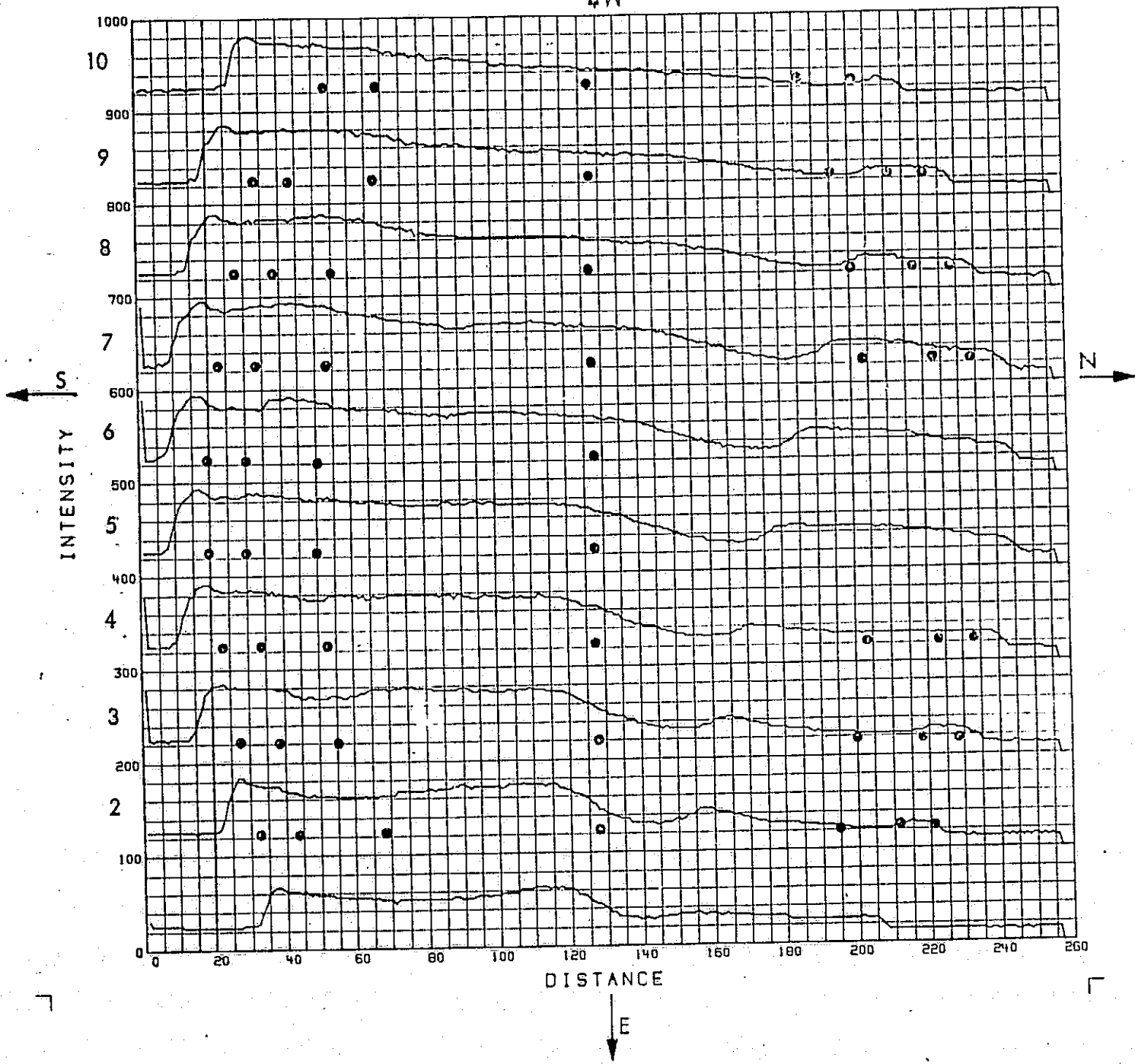


Figure A1

N76-15708

A P P E N D I X C

ATS-5 observations of plasma sheet particles
before the expansion-phase onset.

K. Fujii, A. Nishida

Institute of Space and Aeronautical Science
University of Tokyo
Komaba, Tokyo 153
Japan

R.D. Sharp and E.G. Shelley

Lockheed Palo Alto Research Laboratory
Palo Alto, Calif. 94304
USA

Abstract

Behaviour of the plasma sheet around its earthward edge during substorms is examined by using high resolution (every 2.6 sec) measurements of proton and electron fluxes by ATS-5. In the injection region near midnight the flux increase at the expansion-phase onset tends to lag behind the onset of the low-latitude positive bay by several minutes. Depending upon the case, before the above increase (1) the flux stays at a constant level, (2) it gradually increases for some tens of minutes, or (3) it briefly drops to a low level. Difference in the position of the satellite relative to the earthward edge and to the high-latitude boundary of the plasma sheet is suggested as a cause of the above difference in flux variations during the growth phase.

§ 1. Introduction

One of the characteristic features of the magnetospheric substorm is the enhancement in the population of energetic particles in the magnetosphere. Some of these particles emerge in the high-latitude ionosphere and produce the auroral substorm, while some others are injected into the inner magnetosphere and feed the radiation belts. Past observations on board the ATS satellites have shown that the synchronous orbit at $L = 6.6$ near midnight is an ideal location for monitoring the inflow of these energetic particles from the magnetotail to the radiation belts. Detailed studies have shown that particles are injected first in the slightly pre-midnight region and then drift toward the dayside following an adiabatic trajectory (DeForest and McIlwain, 1971; McIlwain, 1974).

Interest has naturally been attracted to the problem of how these energetic particles are produced in the magnetotail. Coordinated observations of the particle and field environment beyond $\sim 10 R_e$ in the magnetotail have recently confirmed that the magnetic field reconnection that takes place at the distance of somewhere around $15 R_e$ is the essential process that provides energy to the substorm expansion phase (Nishida and Nagayama, 1973; McPherron et al, 1973). The onset of the expansion phase is signified on the ground by, among other things, the appearance of the low-latitude positive bay (Iijima and Nagata, 1972). The comparison of ATS particle observations with ground magnetograms has shown that the enhancement of the energetic particle flux is frequently observed when the expansion phase signature is registered on the ground (Kamide and McIlwain, 1974).

The onset of reconnection tends to be preceded by a gradual deformation of the magnetotail in which field lines are stretched further and the magnetic energy content is increased (Nishida and Nagayama, 1973; McPherron et al, 1973; Maezawa, 1975). The purpose of this paper is to examine the behaviour of energetic particles at the synchronous orbit during this phase, i.e. the growth phase, of substorms. Points of interest include whether or not appreciable injection of energetic particles occurs prior to the expansion phase and how the deformation of the magnetic field affects the particle population observed relatively deep in the magnetosphere. We shall find cases of flux increases like those reported by Shelley et al. (1971) and also see cases of flux decreases as reported by Bogott and Mozur (1973). The observation of the flux increase directly associated with the expansion-phase onset usually lags behind the ground signature.

Data utilized in the present analysis are obtained by Lockheed particle detectors on ATS-5 which survey electrons in the energy range of 0.65 to 3 keV and protons in the energy range of 5 to > 38 keV. In most channels sampling is made twice in each 5.12 sec. A detailed description of the instrument is given in Reed et al. (1969). Table 1 summarizes the energy range of the detectors used in this study and Table 2 contains the geomagnetic coordinates of the ground geomagnetic observatories whose data are reproduced. Reference is also made to the interplanetary magnetic field observations by Explorer 33 and 35.

§ 2. Flux enhancement after the expansion-phase onset

Before proceeding to examine the complex behaviour of the plasma flux occasionally seen before the substorm expansion phase, we shall look at a couple of relatively simple cases. Figure 1 shows the records of electron (EA through ED) and proton (PA through PC) fluxes and of the northward component B_z of the magnetic field observed at ATS-5 in association with a substorm event whose ground signatures are exemplified by low-latitude (Dallas) and auroral-zone (Fort Churchill) magnetograms obtained near midnight. At the onset of the expansion phase indicated by vertical lines the ATS-5 was near the ~ 23 LT meridian. This substorm was an isolated event that followed a quiet interval with K_p of 1-,10.

It is readily seen from Figure 1 that particle fluxes in all the channels started to increase after the onset of the expansion phase was noted on the ground. The high resolution records reproduced in Figure 2 strengthen this observation. The delay of the flux enhancement relative to the expansion-phase onset is about 7 minutes for all the electron channels, about 4 minutes for the lowest-energy proton channel (PA), and about 10 minutes for the other two proton channels. The magnetic field B_z , on the other hand, started to increase nearly simultaneously with the ground observation of the expansion-phase onset. Thus in the present case the arrival of the $1 \sim 30$ keV range plasma at the synchronous orbit near midnight is appreciably delayed from the change in the magnetic configuration of the nightside magnetosphere. Since there is little energy dispersion in the arrival-time of electrons, the longitudinal drift of particles from the "injection region" located far from the point of observation obviously cannot explain the observed time delay.

The next event, Figures 3 and 4, represents an example of relatively simple behaviour of the plasma fluxes observed on the evening side around 19 LT. The format of the figures is the same as before, except that magnetograms from San Juan and Narssarssuaq are used to represent the ground signature of substorms near midnight. The record of the solar ecliptic latitude of the interplanetary magnetic field observed by Explorer 35 is also displayed. The Kp index for the last two 3-hour intervals of the previous day (October 11) was 2- , 2o. At this local time the delay of the electron increase is large (\geq 20 minutes) and energy dependent, and it is probably due largely to the longitudinal drift from the injection region. The delay of the proton increase, on the other hand, is only about 3 minutes and relatively insensitive to energy. The depression in B_z begins nearly simultaneously with the proton flux enhancement. Thus in the present case protons are injected and the magnetic field is disturbed on the evening side at the synchronous orbit a few minutes after the onset of the expansion-phase is observed in the near-midnight region.

We have compared the high resolution data of the ATS-5 particle detector around midnight with ground magnetograms on 12 days in September and October, 1969. In all cases where the signature of the expansion-phase onset is observed in the low-latitude magnetograms, there is a flux increase that seems to be directly associated with it, although the flux variations in the interval preceding the onset differ from case to case as we shall see later. The onset time of such a flux increase is almost always found to be later than the time of the ground signature, including those near-midnight cases where energy dispersion is nearly absent.

§ 3. Injection of low-energy particles before the expansion-phase onset

In the case of the substorm event presented in Figures 5 and 6, the magnetic signatures observed both on the ground and at ATS-5 near the midnight meridian are almost the same as those observed earlier for the simple events in Figures 1 and 2; There is a well-defined auroral-zone negative bay, a low-latitude positive bay, and a B_z increase at ATS-5. (K_p for the previous intervals is 30, 2- .) However, an important distinction is noted in the response of the electron fluxes to this substorm. While in the previous case the electron flux in each of the four channels started to increase well after the expansion-phase onset, in the present case the enhancement is registered in the two low-energy electron channels (detecting electrons in the energy range of 0.65 to 1.9 keV and 1.8 to 5.4 keV respectively) about 15 minutes before the expansion-phase onset. From the high resolution data of Figure 6 it can be seen that the mean energy of electrons increased gradually during this interval, but the flux observed in the highest energy channel ED (observing electrons in the range of 17 to 53 keV) did not rise above background until the onset of the expansion phase.

At the expansion-phase onset a flux enhancement is observed in all the electron and proton channels except the lowest-energy electron channel EA. The magnetic field B_z also rose slightly. A greater increase in the plasma flux is observed, however, about 4 minutes later in coincidence with the sharp increase in B_z . At this time the flux enhancement is more significant in the higher energy channels and the fluxes in the lowest-energy channels PA and EA are even reduced. Thus in contrast to the pre-expansion enhancement which is characterized by a low mean electron energy (< 5

keV), the post-expansion enhancement has a harder spectrum and the mean energy shifts to a higher level.

Another example of a pre-expansion enhancement is given in Figures 7 and 8. ATS-5 was again in the near-midnight (~ 23 LT) region at the onset of a small expansion phase as seen in Figure 7. Kp in the preceding intervals is 0+ , 1- . The enhancement in the electron flux started about 20 minutes before the expansion-phase onset and the mean energy rose gradually although the ED channel remained unaffected. Then, in conjunction with the onset of the expansion phase the flux levels in the high energy channels EC, ED and PC rose, while the low-energy fluxes in EA, EB and PA were little affected. These are essentially the same features as observed in the previous example. The only difference is that the increase in B_z does not accompany the enhancement of energetic particles at the expansion-phase onset and a significant B_z enhancement is observed about 20 minutes later. More examples of this kind can be found in previous publications of Shelley et al. (1971) and Mende et al. (1972).

§ 4. Depression in particle flux before the local onset of the expansion phase

In the event starting from ~ 0912 October 2 1969 shown in Figures 9 and 10 a depression in the plasma flux is clearly recorded in association with the substorm. This event followed a period of high activity with Kp of 4o and 5-. The starting times of the severe decrease and the subsequent recovery of the flux are nearly the same for all energy channels of both particle species, and the start of the B_z increase is roughly coincident with the start of the flux recovery. Since the enhancement in the plasma flux has been found to follow the expansion-phase onset on the ground in the majority of the events, we interpret this recovery of the flux to be a feature that is associated with the onset of the expansion phase. A slightly longer delay (~ 12 minutes) of the flux increase from the ground signature for the present event as compared to other cases is probably related to the ATS-5 location in the post-midnight sector at ~ 02 LT; the expansion-phase onset time is determined in this case by the evening side data (Guam and Honolulu) where the low-latitude positive bay is first recorded. The depression in the plasma flux lasting for ~ 5 minutes is then interpreted to be the feature that precedes the local onset of the expansion phase.

Another example which is probably of a type similar to the previous one is the 0607 September 15, 1969 event presented in Figures 11 and 12. In this case, which also followed an interval of high Kp (4o, 4-), the sharp rise in flux, which is observed in all channels to start about 4 minutes after the expansion-phase onset, is preceded by a gradual decrease that lasts for ~ 15 minutes from ~ 0550. Although gradual flux decreases may generally be attributed to a mere decay from a higher level produced

by the earlier injection, the fact that the flux decrease started, or the rate of the decrease became higher, nearly simultaneously for both species in all channels makes decay due to a drift motion out of the injection region untenable as an explanation. For flux decreases as observed on October 2 and September 15 a mechanism must be operative that affects the entire particle population in the $1 \sim 100$ keV range.

In the cases where the flux prior to the advent of the substorm event concerned is at an enhanced level characteristic of the plasma sheet, the flux enhancement at the expansion phase onset is very frequently preceded by a flux depression. Reflecting, probably, the fact that the earthward edge of the proton plasma sheet is located closer to the Earth than that of the electron plasma sheet (Frank, 1967; Schield and Frank, 1970), the frequency with which protons are seen at these enhanced levels is higher than that of electrons at the synchronous orbit on the nightside. Hence, the chances of observing the flux depression prior to the expansion-phase onset is higher for protons, and cases of proton flux depressions lasting for ~ 1 hour or more can be found in the events presented in Figures 5, 9 (third event), and 11 (both events). It is noted that the onset time of the proton flux depression in the October 18 event (Figure 5) depends little on energy, and some of these depressions may also be due to processes other than escape by azimuthal drift.

5. Discussion

At the onset of the expansion phase when the neutral line is formed in the near-tail region, field lines and associated plasma earthward of the neutral line swings back toward the Earth (Nishida and Nagayama, 1973). The intensification of the plasma flux that is observed shortly after the expansion-phase onset is likely to be due to this motion of the plasma sheet. At the same moment the poleward motion of the auroral arc is usually observed at ionospheric heights, but this poleward motion is probably related to the process that takes place far beyond the earthward edge of the plasma sheet, since the diffuse aurora, which is considered to be the projection of the plasma sheet, occupies a wide latitudinal range equatorward of the discrete aurora (Lui et al., 1975).

The flux increase directly associated with the expansion-phase onset tends to occur after the first detection of the expansion-phase signature on the ground. As can be seen in Figures 2, 6, 8 and 12, this applies to flux increases that are observed near midnight in the injection region where the times of the flux increases depend little on energy. If we take five minutes as a typical value of the time lag, the distance traveled by those particles constituting the front of the above flux increase is given by $3 \times 10^5 E/B$ km where E is in mV/m and B is in gammas. With typical values of $E \sim 1$ mV/m and $B \sim 60 \gamma$, this gives 5×10^3 km $\approx 0.8 R_E$. Thus the hot plasma reaching the synchronous altitude at the expansion-phase onset appears to come from a relatively close vicinity rather than from the neutral line formed at the distance of $\approx 5 R_E$ beyond the synchronous altitude. Betatron and Fermi type accelerations associated with the contraction of the nightside magnetic field lines would be principal mechanisms for produc-

ing the surge of the hot plasma. That increases in flux and field (B_z) do not always occur together at the synchronous altitude can be understood because the field variations can travel faster and spread more widely as waves than the particle streaming.

As suggested by Shelley et al. (1971) the enhancement of low-energy electrons, probably of plasma sheet origin, prior to the expansion-phase onset could also be due to the earthward displacement of the inward edge of the plasma sheet. The dawn-to-dusk electric field that causes the earthward drift of the nightside magnetospheric plasma has been found to increase during the growth phase of substorms (Mozer, 1971). The origin of this electric field lies in the interaction process at the magnetopause. Nevertheless, some conditions have to be satisfied for the flux increase to occur at the synchronous altitude. As field lines are stretched away during the growth phase a dusk-to-dawn electric field is generated in the tail. The strength of this reverse electric field must be less than that of the dawn-to-dusk electric field at the inward edge of the plasma sheet; otherwise, the entire plasma sheet would move away from the earth following the stretching of the tail field lines. Also, the inward edge must be originally located close enough to the synchronous altitude. If particles started their inward motion from too great a radial distance, they would be energized on the way in by the conservation of the first two invariants, and could be forced to drift sideways across $\text{grad } |E|$ before reaching the synchronous altitude. The imposition of these conditions could be the reason why the pre-expansion increase of the electron flux is not always observed.

As for the flux decrease preceding the expansion phase, Bogott and Mozer (1973) found numerous cases of the same kind in their 30 - 300 keV electron observation on ATS-5. Since the energy range of their detector

corresponds to radiation belt electrons, they suggested the inward motion of the trapping boundary as the explanation. Such an inward motion would indeed occur for trapped particles whose trajectories are governed by the $\underline{v}_B \times \underline{B}$ drift, since the stretching of the field lines leads to a reduction of the magnetic field strength in the nightside, inner magnetosphere and to a shrinkage of the drift shells during the growth phase. However, our present observations reveal that a flux decrease occurs also for very low-energy particles which are most likely to belong to the plasma sheet whose distribution is centered outside the synchronous altitude. Since at low energies the $\underline{v}_B \times \underline{B}$ drift speed is relatively small and the electric field is the dominant factor that governs the drift motion, the decrease in the low-energy particle flux has to be caused by electric field variations. A possibility that must be considered is that the low-energy plasma is transported away from the earth by the stretching field lines. For this to be the case it is required that the dusk-to-dawn electric field associated with the stretching of field lines is stronger, even at the synchronous altitude, than the dawn-to-dusk electric field produced by the interaction process working at the magnetopause. Another possibility is that the flux decrease is due to a thinning of the plasma sheet as described by Hones et al. (1973). The ATS-5 satellite at 105° W longitude is approximately 10° above the geomagnetic equator so that a sharp reduction in the width of the plasma sheet at $6.6 R_E$ could bring the satellite close to the boundary with the upper lobe of the tail. The idea that plasma sheet thinning occurs during the growth phase at the radial distance as deep as $L \sim 8$ has also been suggested by Kivelson et al. (1973) and Buck et al. (1973).

If the depression in the proton flux observed on October 18 (Figure 5) is not entirely due to the loss by the azimuthal drift but to the process sought above, the first possibility, namely the anti-earthward motion of the plasma, has to be eliminated since the low-energy electrons are being intensified at the same time when the proton flux is depressed prior to the expansion-phase onset. The second possibility, namely the thinning of the plasma sheet, would not contradict the observation, however, as the proton flux does not drop to the background level; the satellite could be located inside the thinning but earthward-extending plasma sheet.

Acknowledgement

Part of the work was supported by NASA under the Contract NASw 2656. Explorer 33 and 35 magnetic field data are obtained from WDC-A, Rockets and Satellites.

References

- Bogott, F.H. and Mozer, F.S. (1973), J. Geophys. Res. 78, 8119.
- Buck, R.M., West., J.I., Jr. and D'Arcy, R.G., Jr. (1973). J. Geophys. Res. 78, 3103.
- DeForest, S.E. and McIlwain, C.E. (1971). J. Geophys. Res. 76, 3587.
- Frank, L.A. (1967). J. Geophys. Res. 72, 1905.
- Iijima, T. and Nagata, T. (1972). Planet. Space Sci. 20, 1095.
- Kamide, Y., and McIlwain, C.E. (1974). J. Geophys. Res. 79, 4787.
- Kivelson, M.F., Farley, T.A., and Aubry, M.P. (1973). J. Geophys. Res. 78, 3079.
- Lui, A.T.Y., Anger, C.D., and Akasofu, S.-I. (1975). J. Geophys. Res. 80, ****.
- Maezawa, K. (1975). Planet. Space Sci. 23, ****.
- McIlwain, C.E., (1974). in Magnetospheric Physics, ed. B.M. McCormac, D. Reidel Pub. Co., 143.
- McPherron, R.L., Russell, C.T. and Aubry, M.P. (1973). J. Geophys. Res. 78, 3131.
- Mende, S.B., Sharp, R.D., Shelley, E.G., Haerendel, G. and Hones, E.W., Jr. (1972). J. Geophys. Res. 77, 4682.
- Mozer, F.S. (1971). J. Geophys. Res. 76, 7595.
- Nishida, A. and Nagayama, N. (1973). J. Geophys. Res. 78, 3782.
- Reed, R.D., Shelley, E.G., Bakke, J.C., Sanders, T.C., and McDaniel, J.D. (1969). IEEE Trans. Nucl. Sci. NS-16, 359.
- Schild, M.A., and Frank, L.A. (1970). J. Geophys. Res. 75, 5401.
- Shelley, E.G., Johnson, R.G., and Sharp, R.D. (1971). Radio Sci. 6, 305.

TABLE 1. Energy Ranges of Detectors

Channel Name	Particle	Energy Range, KeV
EA	e	0.65 - 1.9
EB	e	1.8 - 5.4
EC	e	5.9 - 17.8
ED	e	17.4 - 53
PA	P	> 5
PB	P	> 15
PC	P	> 38

TABLE 2. Geomagnetic Observatories

	Geomag. latitude	Geomag. longitude
Narssarssuaq	71	37
Fort Churchill	69	323
Sitka	60	275
Dallas	43	328
San Juan	30	3
Honolulu	21	266
Guam	4	213

Figure Captions

1. Particle and field observations by ATS-5 during a substorm event.

LEFT PANEL: electron flux.

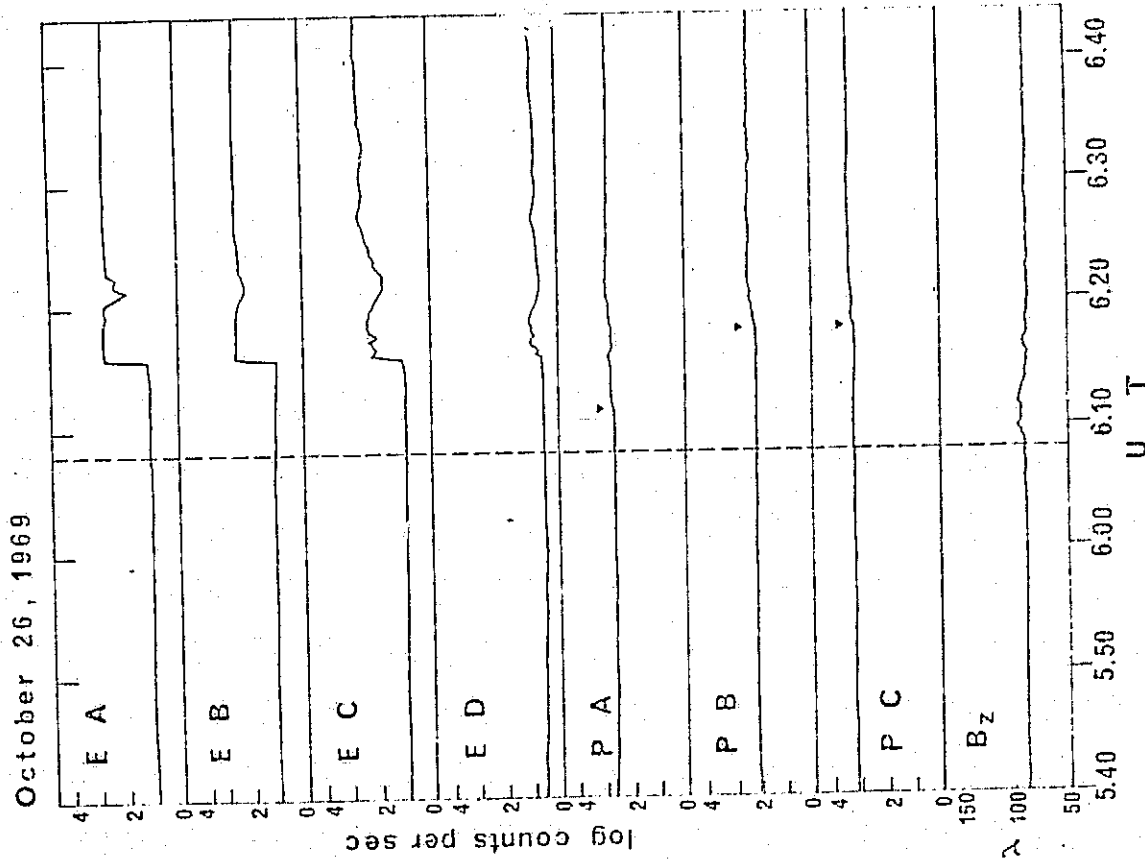
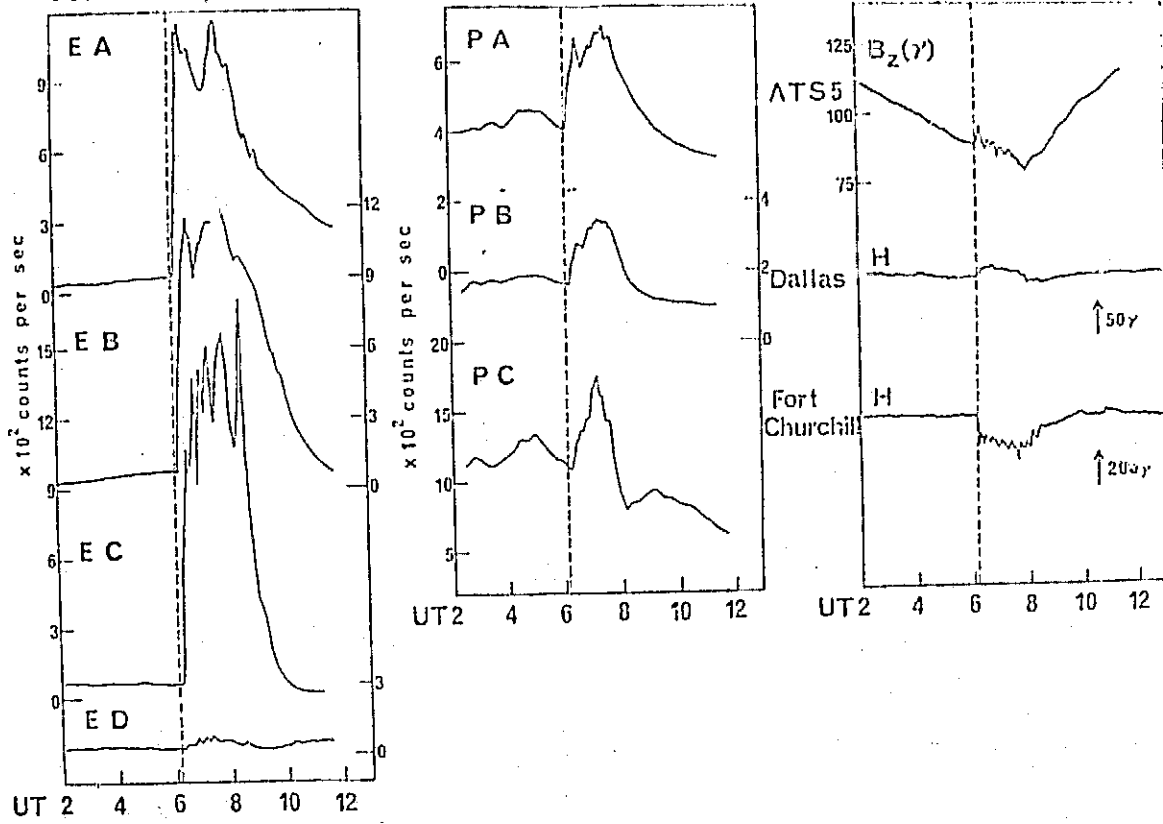
MIDDLE PANEL: proton flux.

RIGHT PANEL: northward component of the magnetic field, and ground magnetogram data for reference.

The onset time of the expansion phase is determined by the night-time, low-latitude positive bay and is indicated by vertical dashed lines.

2. High resolution data plot corresponding to the event of Figure 1. Wedge marks emphasize onsets of proton enhancements.
3. ATS-5 particle and field data similar to Figure 1. Shadings indicate the interval in which ATS-5 was in the Earth's shadow. Interplanetary magnetic field data (solar magnetospheric latitudinal angle) are given at bottom, right.
4. High resolution data plot corresponding to Figure 3.
5. ATS-5 particle and field observations and reference data. Similar to Figure 3.
6. High resolution data plot corresponding to Figure 5.
7. Similar to Figure 5.
8. High resolution data plot corresponding to Figure 7.
9. ATS-5 particle and field observations for a series of substorm events. The second event is chosen for examination in the text.
10. High resolution data plot corresponding to the second event of Figure 9.
11. Similar to Figure 9.
12. High resolution data plot corresponding to the second event of Figure 11.

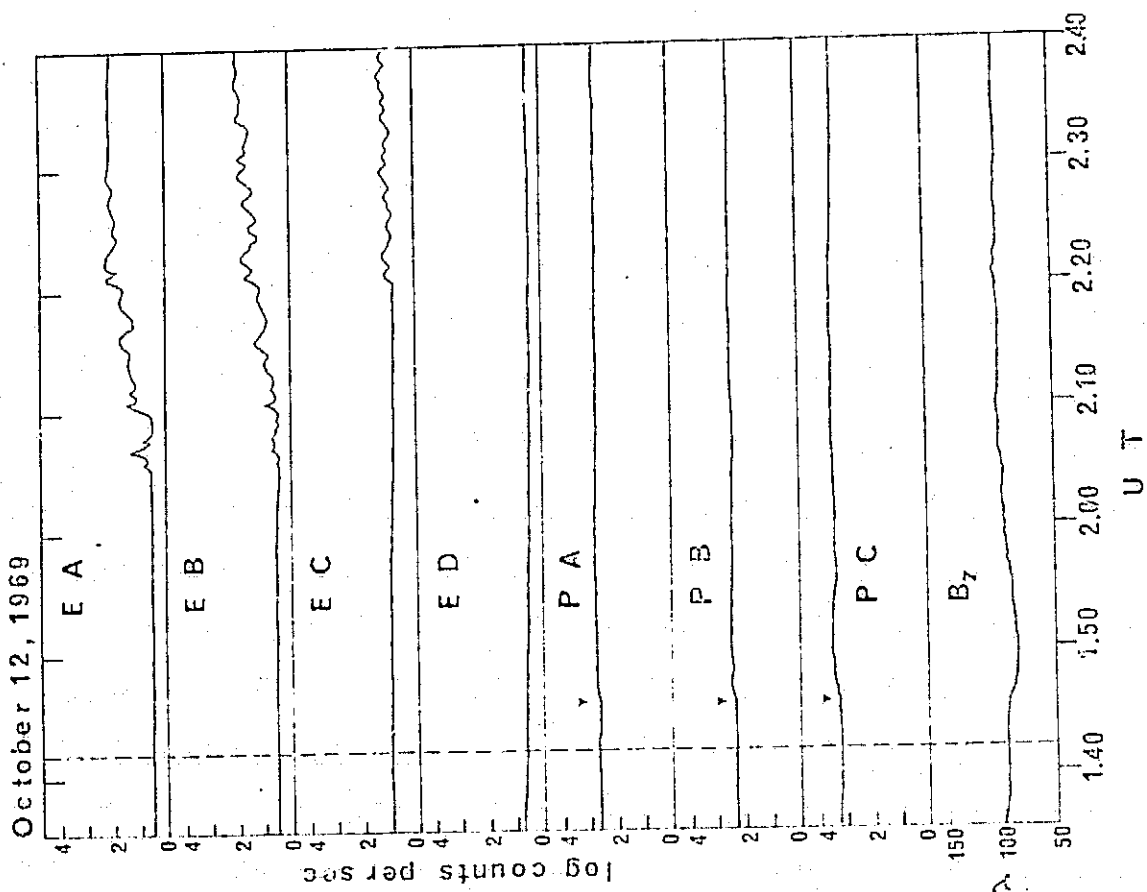
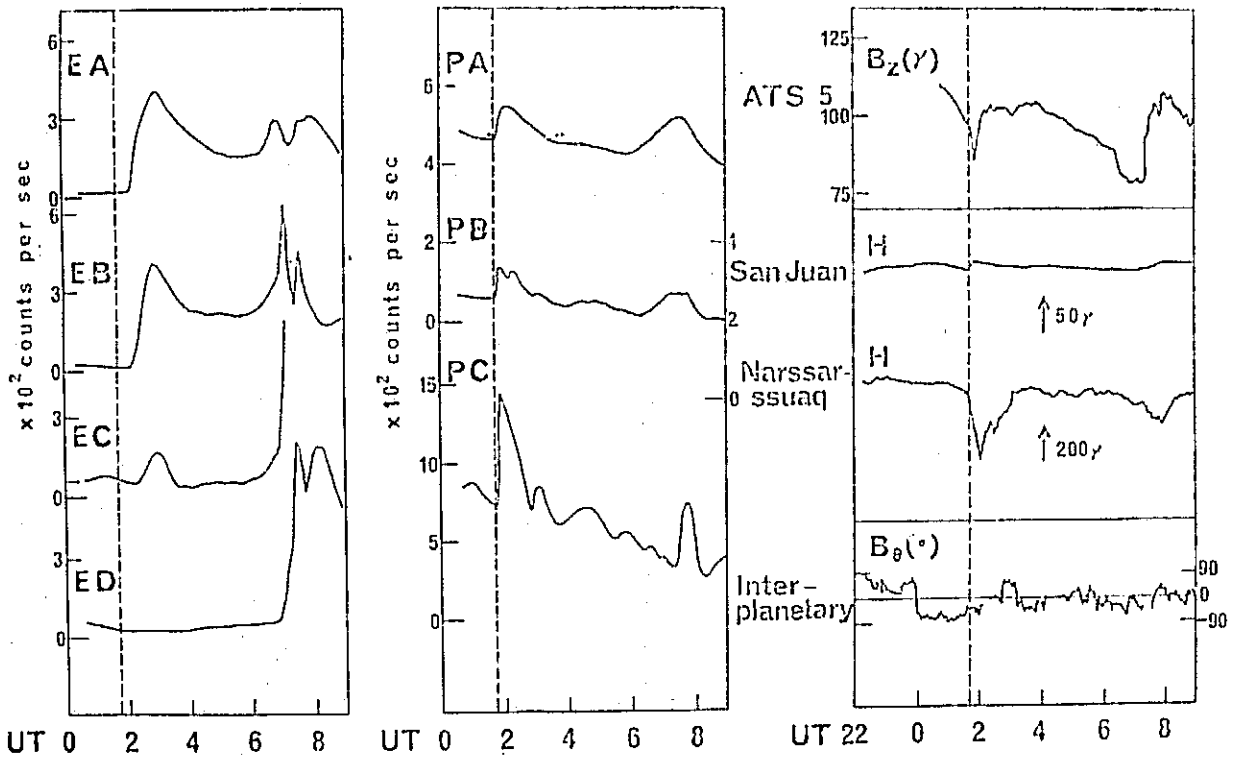
October 26, 1969



(2)

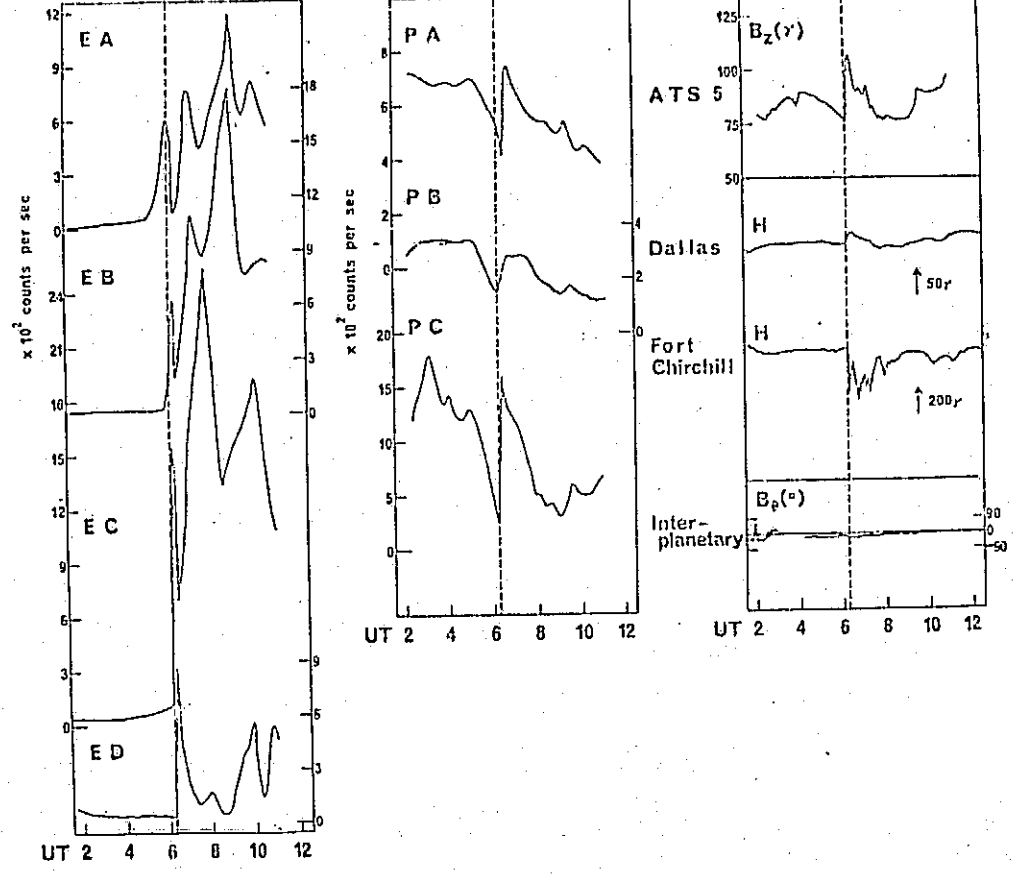
PRECEDING PAGE BLANK NOT FILMED

October 12, 1969

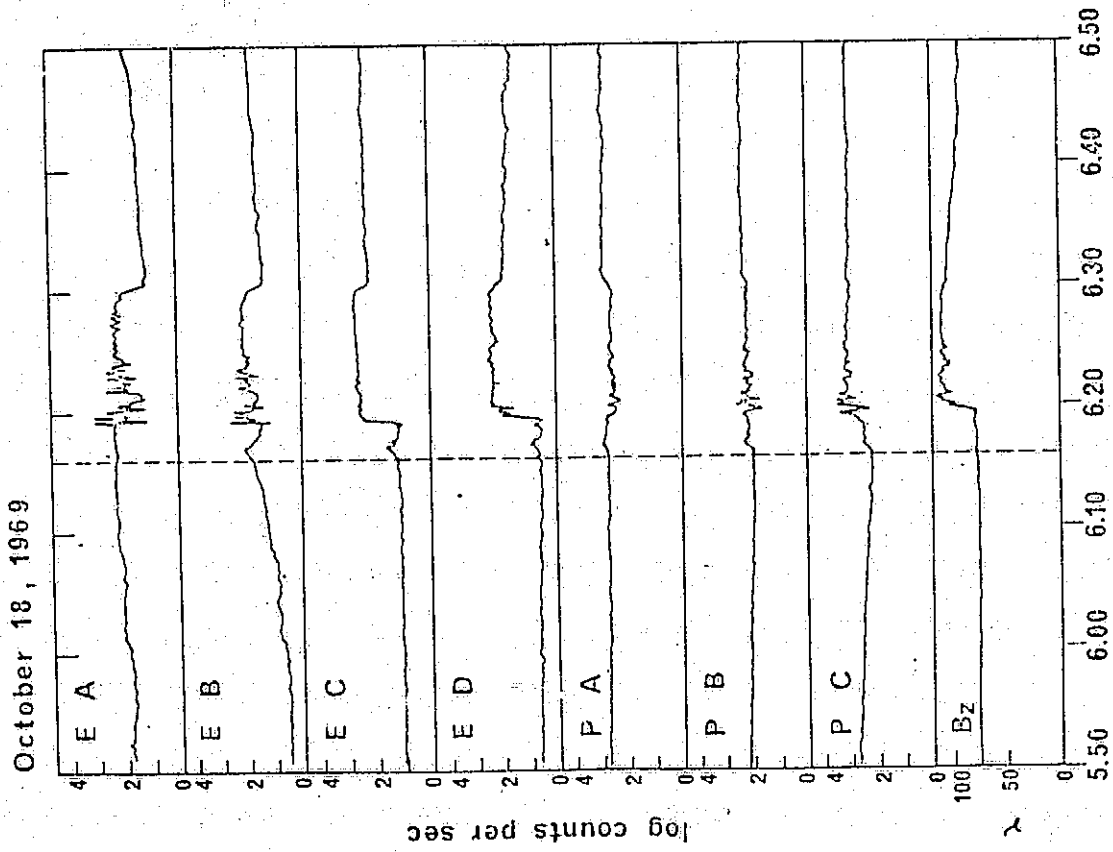


4

October 18, 1969

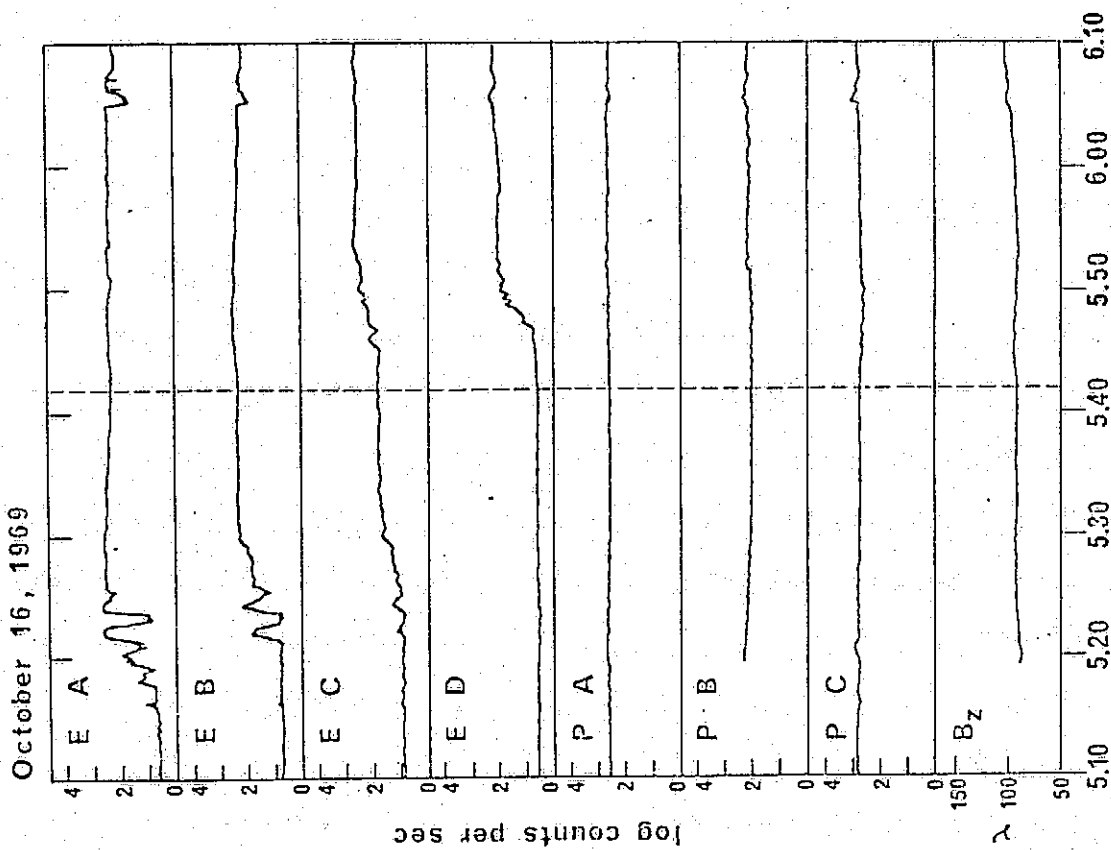
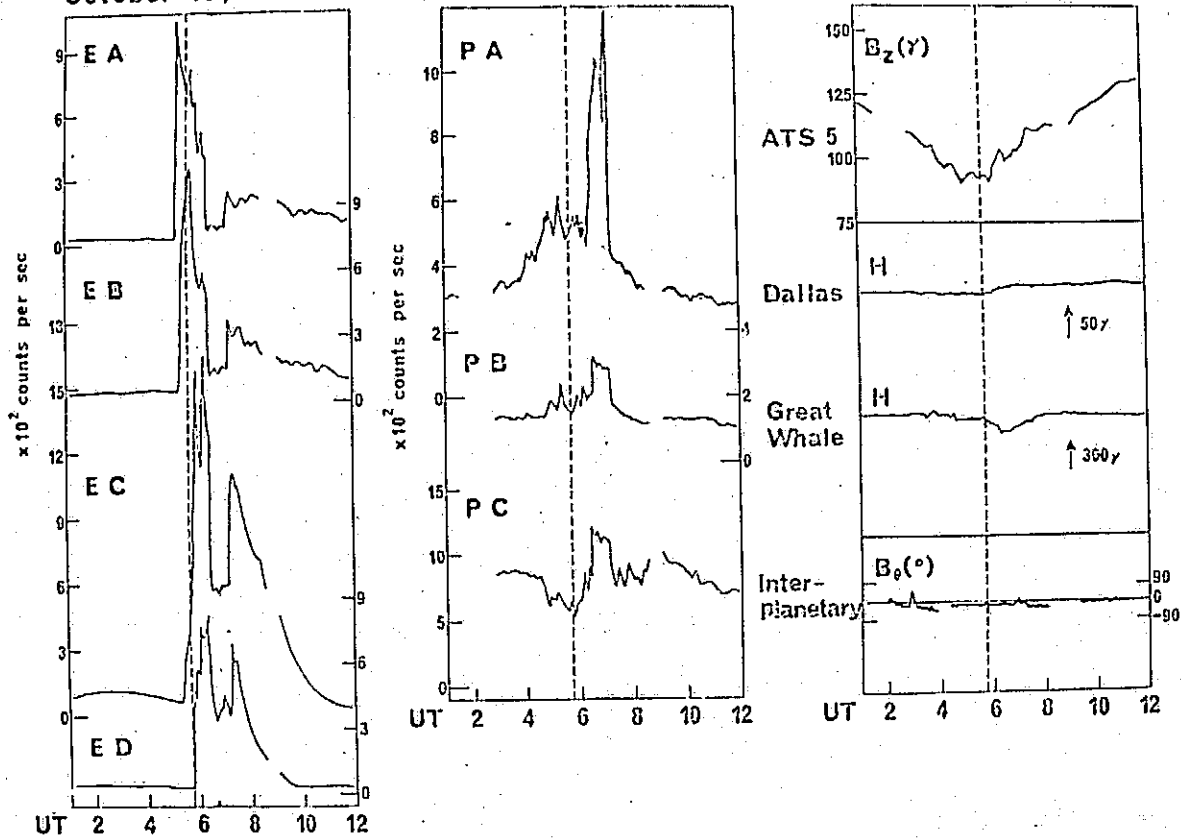


6

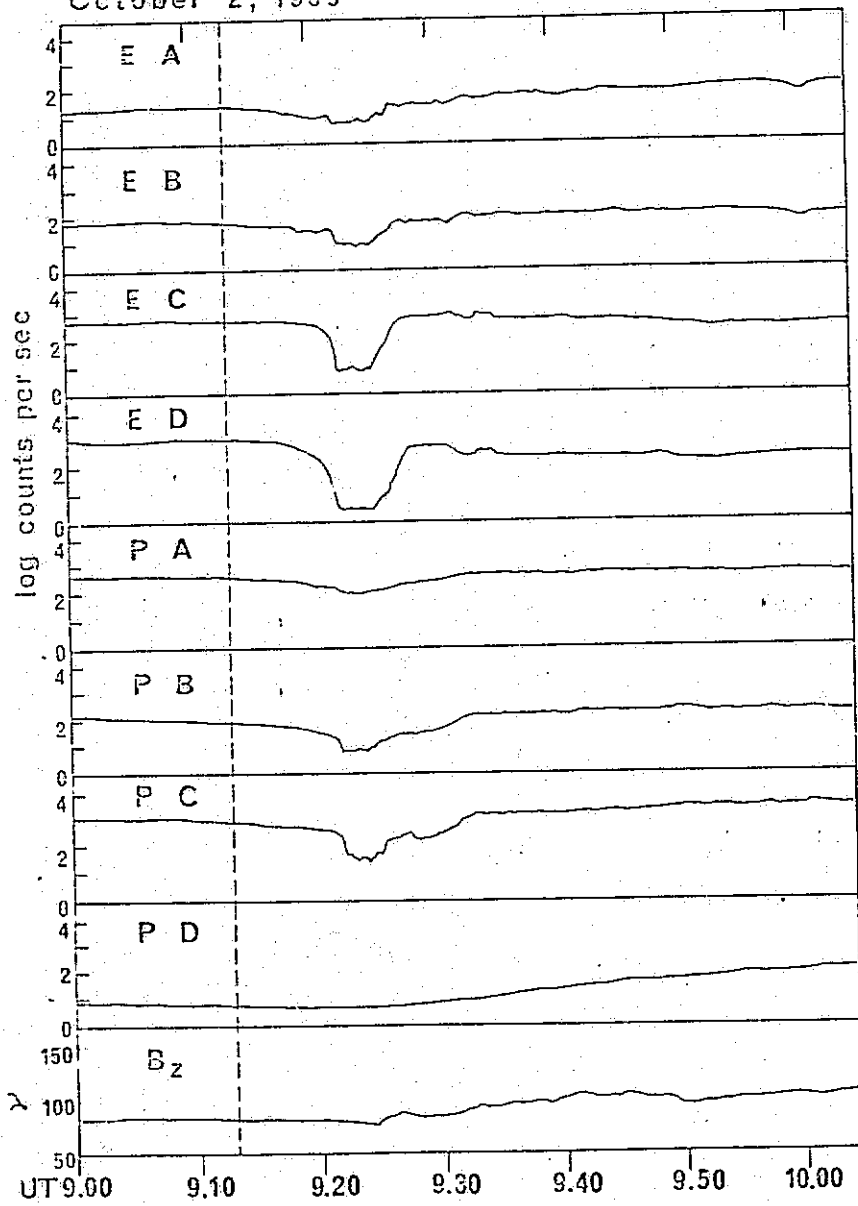


C.2

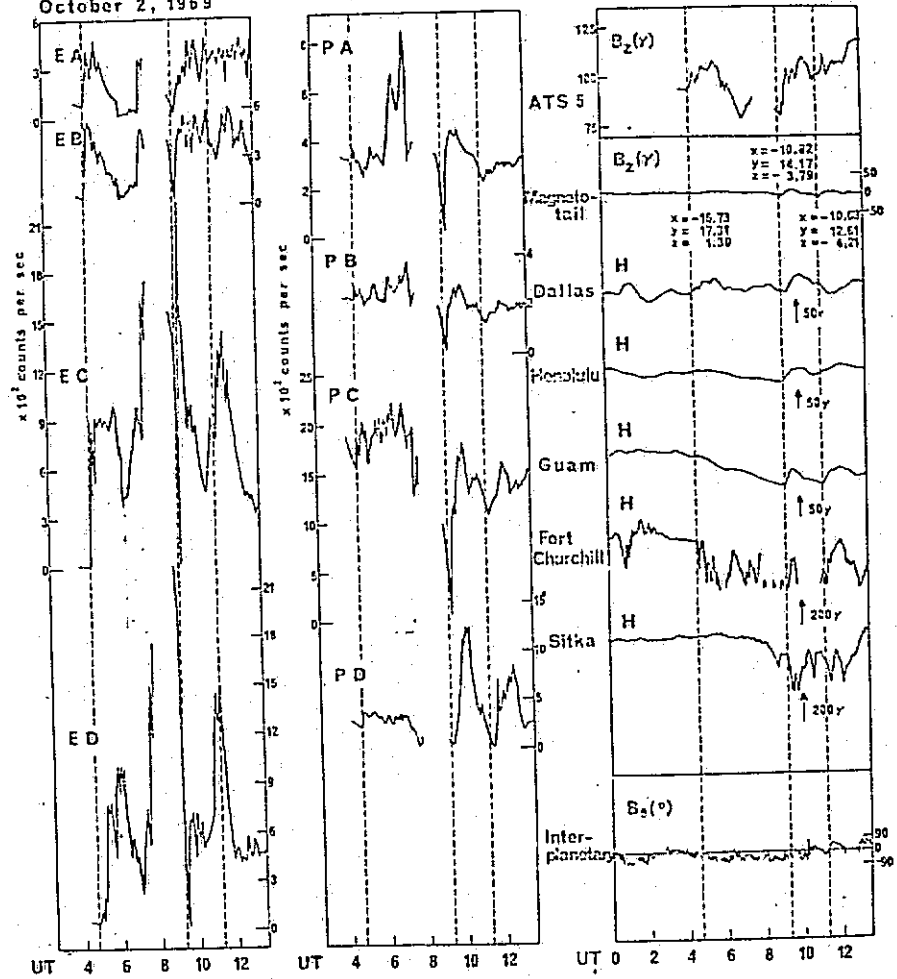
October 16, 1969

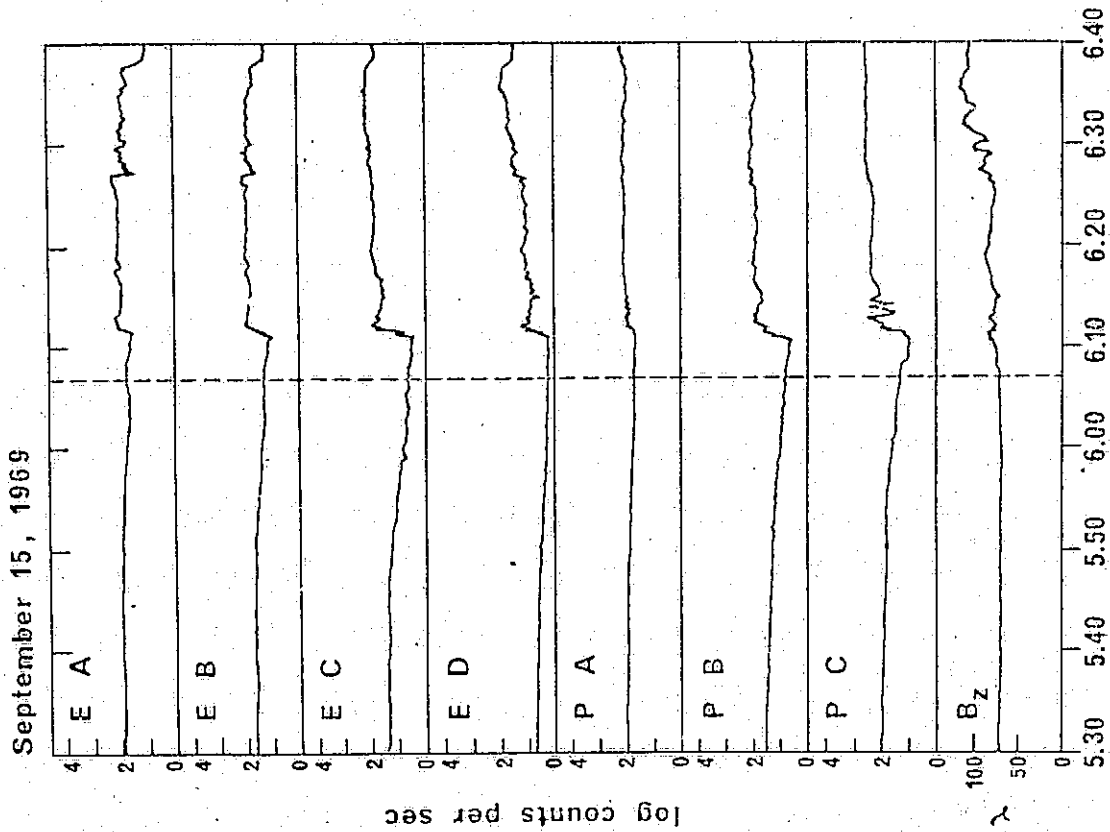
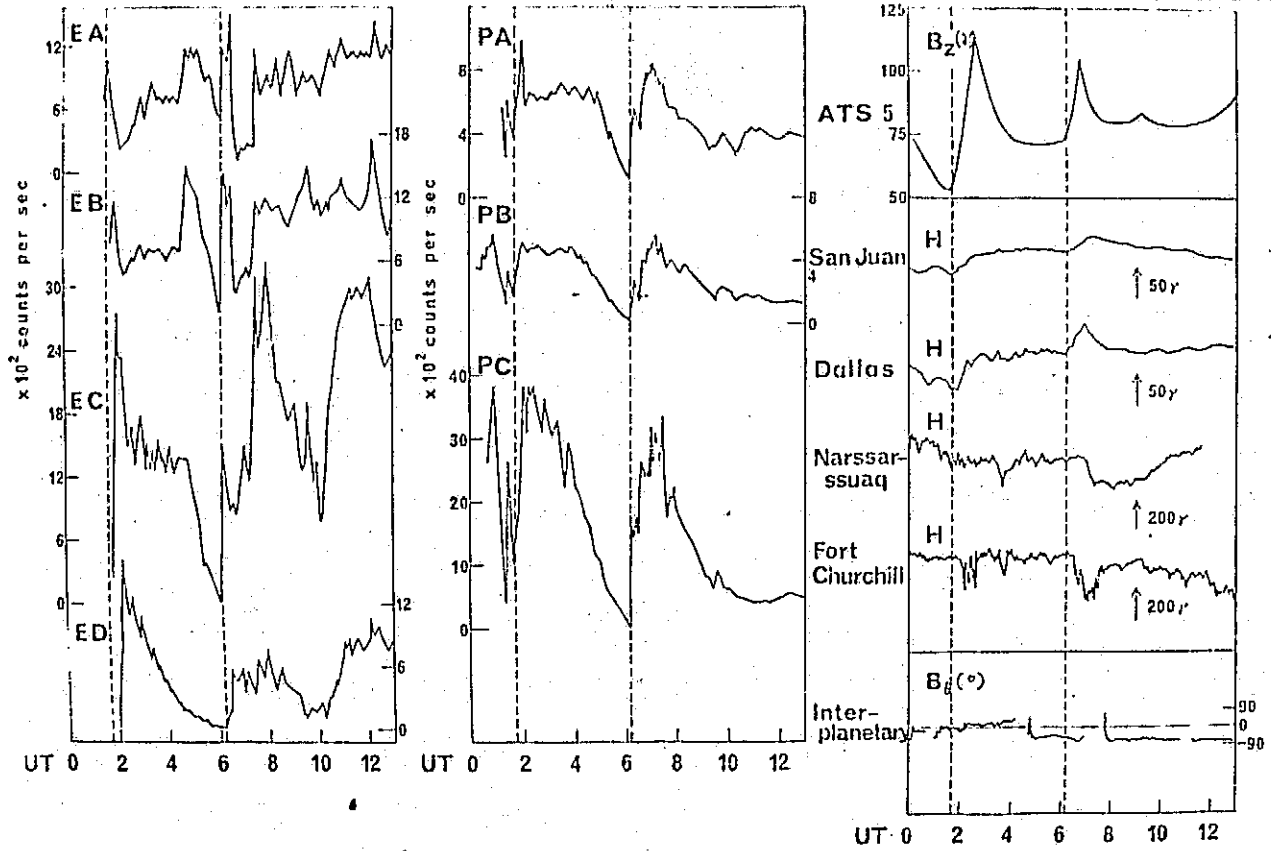


October 2, 1969



October 2, 1969





12

A P P E N D I X D

A COMPREHENSIVE STUDY OF SUBSTORM SEQUENCES
ON SEPTEMBER 8, 1969

G. Rostoker, S.-I. Akasofu, H. Fukunishi, E. W. Hones, Jr.,
L. J. Lanzerotti, C. G. MacLennan, R. L. McPherron,
R. D. Sharp, and R. G. Wiens

ABSTRACT

Recent studies of magnetospheric substorms have yielded the fact that their macrostructure involves quasi-periodic intensifications of electrojet strength with each intensification being the signature of the creation of a new element of the electrojet. In general, it is found that each new element lies to the north and west of the preceding one. A series of such intensifications terminated by the creation of the most westerly current element will be termed a substorm sequence. The significance of the terms "magnetospheric substorm" and "polar magnetic or auroral substorm" will be discussed in the context of this morphology.

Particle and field responses measured in the ionosphere and magnetosphere during the course of magnetospheric substorms are found to be highly complex, with various signatures being observed which appear to be a function of local (magnetic) time and the position of the monitoring satellite with respect to the field lines on which the disturbance is taking place. For the most part, substorm signatures in space have been studied using different suites of substorm data for each relevant satellite, with multiple satellite studies of a single event being rare. In this study, we present a detailed analysis of a series of substorm sequences which occurred during the first half of the UT day September 8, 1969. Ground-based magnetometer data consisted of the normal magnetograms from the worldwide network supplemented by data from the University of Alberta station and from the Tungsten observatory operated by UCLA. All-sky camera data were available from some Canadian and Alaskan high-latitude observatories. Interplanetary solar wind and magnetic field data were recorded by the Explorer 35 satellite, while magnetotail particle data were supplied by the VELA satellite and the magnetic field by the OGO-5 satellite. Information at synchronous orbit was provided by the ATS-1 and ATS-5 geostationary satellites and consisted of magnetometer and energetic particle data.

Ground-based magnetograms were used to define the times of substorm intensifications and the various particle and magnetic field variations at each satellite were coordinated in the framework of the ground-based observations. In the magnetotail it is found that the plasma sheet responds very sensitively to substorm intensifications, with signatures being noticeable in terms of thinning and thickening as well as changes

in the hardness of the energy spectrum. At synchronous orbit, the injections, modulations and drifts of the electron and proton fluxes are discussed with reference to the position of the satellite with respect to the longitudinal extent of the substorm disturbed region.

The study presented in this paper will conclusively demonstrate the importance of knowing the position of both satellites and ground-based observatories with respect to the substorm disturbed region of the magnetosphere if one is to properly interpret the various signatures of the particles and fields during the various phases of magnetosphere storm and substorm activity.

A P P E N D I X E

SIMULTANEOUS OBSERVATIONS OF SYNCHRONOUS-ALTITUDE PARTICLE FLUXES AND THE AURORAL ELECTROJET

R. D. Sharp, E. G. Shelley, and G. Rostoker

ABSTRACT

The magnetospheric substorm at 0700 UT on September 1, 1970 is illustrative of a technique which can be utilized to map geomagnetic field lines from the ionosphere to the equatorial synchronous orbit at 6.7 R_E . Simultaneous data from the University of Alberta magnetometer chain and the Lockheed auroral particle spectrometer on ATS-5 provide the basis for this type of study. The expansive phase of the substorm in question was initiated at low latitudes and no simultaneous effects were observed at ATS-5. A typical poleward expansion of the electrojet followed, with a sudden increase in the particle fluxes and magnetic field at ATS-5 occurring as the northern border of the electrojet reached $66^\circ \pm 1/2^\circ$. The lack of time dispersion in the onset of the observed responses in the various energy electron channels demonstrates that this was not a longitudinally drifting plasma cloud intercepting the satellite. It is interpreted as a poleward propagating disturbance whose high-latitude edge maps to the location of the northern border of the electrojet. Having established the ground station corresponding to the location of the ATS-5 field line at this point in the substorm, the temporal variation of the electrojet at this location was compared with the particle and magnetic field measurements at synchronous altitude. For about a ten-minute period, associated with the flux increase at ATS-5, there was an apparent correspondence between the amplitude of the electrojet, the electron energy flux at ATS-5, and the rate of re-configuration of the geomagnetic field in the magnetotail, as measured by the variation of the inclination of this field at ATS-5. Additional examples of this type of correspondence have been discovered in other events. A possible interpretation of these results will be explored in terms of a quasistatic convection electric field leading to electrojet polarization and a Cowling current[†] whose amplitude is controlled by the degree of ionospheric conductivity established by the precipitating auroral electrons.

[†]Coroniti, F. V., and C. F. Kennel, "Polarization of the Auroral Electrojet," J. Geophys. Res., 77, No. 16, 2835, 1972.